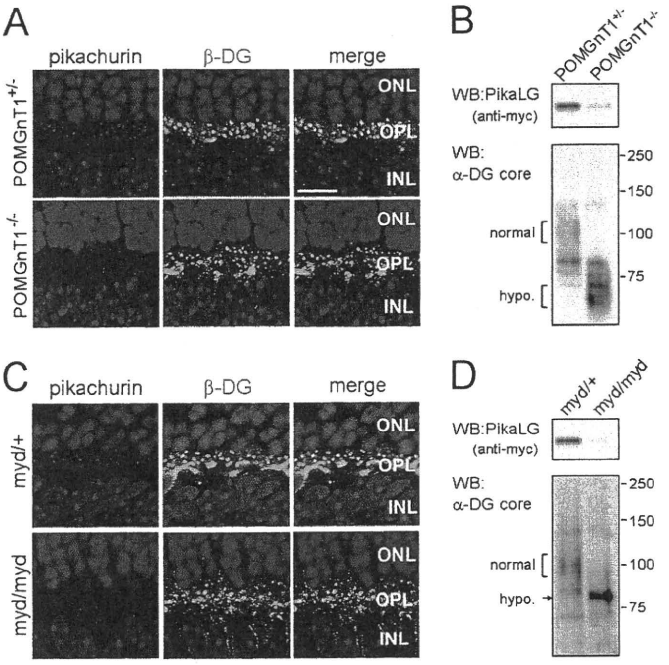

FIGURE 5. **Disruption of pikachurin localization in dystroglycanopathy animals.** *A* and *C*, immunofluorescence analysis of pikachurin in the outer plexiform layer (*OPL*). Retinal sections of *POMGnT1*-deficient (−/−) and *Large*^{myd} (myd/myd) mice, and their littermate heterozygous controls, were immunostained using antibodies to pikachurin (*red, left panels*) or β-DG (*green, middle panels*). Nuclei were stained with DAPI (*blue*). Merged images are shown in the *right panels*. *Scale bar*, 10 μm. *ONL*, outer nuclear layer; *INL*, inner nuclear layer. *B* and *D*, reduced pikachurin binding to α-DG in dystroglycanopathy models. α-DG was immunoprecipitated from eyes of *POMGnT1*-deficient (−/−) and *Large*^{myd} (myd/myd) mice, and their littermate heterozygous controls. PikaLG-containing cell lysates were incubated with the immunoprecipitated materials to examine PikaLG-DG binding. PikaLG binding was detected by Western blotting (*WB*) with anti-Myc antibody (*upper panel, PikaLG*). Comparable amounts of α-DG were confirmed by Western blotting with anti-α-DG antibody (*lower panel, α-DG core*). Normal and hypoglycosylated (*hypo.*) sizes of α-DG are indicated on the *left side* of the blots.

tains an Asp residue equivalent to Asp-2982 in the laminin α2-chain LG5, but they lack a residue equivalent to Asp-3055 (supplemental Fig. 4). The residue equivalent to Asp-3055 in pikachurin LG3 is Asn, which is capable of coordinating a Ca^{2+}, but LG1 and LG2 appear to lack the second Ca^{2+}-coordinating site. It has been shown that a single LG domain is usually insufficient for α-DG binding except laminin α1-chain LG4. This is also the case for pikachurin (Fig. 2). Thus, the adjacent tandem LG2-LG3 domains likely allow multiple Ca^{2+} sites to form a stable pikachurin-DG connection, as is proposed for other known ligand proteins (32). Interestingly, our data show that pikachurin can form oligomeric structures. This suggests the possibility that multimerization or clustering effects may play a role in modulating pikachurin-DG interactions in the native environment.

Unlike the laminin α1-chain and agrin (28, 29), the interaction of pikachurin with α-DG was relatively less sensitive to the inhibitory effects of heparin, although pikachurin LG domains have heparin binding capacity (Fig. 1). Heparin insensitivity at the submilligram/ml range is also observed with the laminin α2-chain and perlecan (33). These data may indicate that the α-DG-binding site is spatially distinct from the heparin-binding site in pikachurin LG domains, thus preventing heparin interference with the α-DG interaction. More interestingly, whereas 0.5 M NaCl strongly inhibits interaction between α-DG and other ligand proteins (33), only a modest inhibitory effect was observed for 0.5 M NaCl with pikachurin-DG binding. The strong inhibitory effects of NaCl on other DG ligand proteins indicate that, in addition to Ca^{2+}-mediated contact, an electrostatic effect may contribute partially to DG-ligand interactions. However, this may not be the case for pikachurin. Rather, it is likely that the Ca^{2+}-binding site in pikachurin primarily ensures the interaction with α-DG. There seem to be subtle differences between the binding of pikachurin to α-DG and that described for other LG domain proteins. Our ligand competition experiments show that PikaLG inhibits laminin-111 binding to DGFc, but even very high concentrations of laminin-111 do not inhibit PikaLG-binding to DGFc (supplemental Fig. 5). These data suggest that pikachurin might contain more binding sites on α-DG than does laminin-111. Alternatively, PikaLG might have much higher affinity for α-DG compared with laminin-111. Further investigation is necessary to reveal pikachurin-binding sites on α-DG in the future.

It is known that certain glycosylation events are necessary for α-DG ligand binding activity; however, the exact glycan structure necessary for the ligand binding is still not determined. Several lines of evidence have shown that among heterogeneous glycans on α-DG, *O*-mannosylation is an essential post-translational modification. The POMT1/2 complex catalyzes the initial Man transfer to Ser/Thr residues (9), and POMGnT1 synthesizes the GlcNAc-β1,2-branch on *O*-Man (12). A very recent study demonstrated the involvement of LARGE in the synthesis of phosphodiester-linked glycan on *O*-Man, which would serve as a laminin-binding moiety (13). Another study showed that β3GnT1 is involved in LARGE-dependent modification (34). β3GnT1 interacts with LARGE, and reduced expression of β3GnT1 leads to diminished synthesis of laminin-binding glycans. Here we have demonstrated that post-translational modification on *O*-Man mediated by LARGE and POMGnT1 is necessary for the pikachurin-DG interaction.

Mutations in these glycosylation pathways are causative for dystroglycanopathy, which is frequently associated with eye involvement, including abnormal retinal physiology. Several models for dystroglycanopathy, including *POMGnT1*-deficient, *Large*-mutant *Large*^{myd}, and *Large*^{vls} mice, show abnormal retinal physiology such as attenuation or delay in the electroretinogram b-wave (23, 24, 35). Previously, we reported that genetic disruption of pikachurin causes an ERG abnormality similar to those seen in other dystroglycanopathy model mice (22). In the retina, DG is expressed in the Müller glial end feet at the inner limiting membrane, in the glial end feet abutting the vasculature (36), and at ribbon synapses of photoreceptors in the outer plexiform layer (37–40). On the other hand, pikachurin localization is specific to the synaptic cleft of the photoreceptor ribbon synapse in the outer plexiform layer (22). In this study, we demonstrated that the pikachurin-DG interaction and pikachurin localization at the ribbon synapse are both disrupted in dystroglycanopathy animals. We propose that proper localization of pikachurin at the ribbon synapse, which is supported by functionally mature DG, plays important roles in the physiology of the retina.

Another physiological role of DG in the retina, apart from the ribbon synapse, was recently demonstrated (7). In that study, it has been shown that deletion of DG in the central nervous system (CNS) causes attenuation of the b-wave, which is associated with a selective loss of dystrophin and Kir4.1 clustering in glial end feet. Dystrophin is the product of the causative gene for Duchenne and Becker muscular dystrophies; it forms a protein complex with DG termed the dystrophin-glycoprotein complex. Loss of either dystrophin or DG results in reduction of the entire dystrophin-glycoprotein complex from the cell surface membrane (2, 41). Importantly, abnormalities in ERG similar to those seen in CNS-selective DG-deficient mice are frequently observed in individuals with Duchenne/Becker muscular dystrophy (42, 43). Dystrophin isoforms generated through differential promoter usage and alternative splicing are regulated in a tissue-specific and developmental manner. Dp260, which is transcribed using an internal promoter, is a retina-specific isoform located in the outer plexiform layer (44). In Dp260-disrupted mice, DG expression in the outer plexiform layer is severely reduced, and the implicit time of the b-wave is prolonged (45). These changes are also observed in dystroglycanopathy and pikachurin-deficient mouse models. Combined with our present work, these studies support the hypothesis that DG contributes to retina function via multiple mechanisms (7), including the pikachurin-DG-Dp260 molecular complex at the ribbon synapse and the DG-dystrophin-Kir4.1 clusters at glial end feet. Overall, our data not only shed light on the molecular pathogenesis of eye abnormalities in muscular dystrophy patients but also contribute to understanding the molecular mechanisms for ribbon synapse formation and maintenance.

Acknowledgments—We thank past and present members of the Toda laboratory for fruitful discussions and scientific contributions. We also thank Chiyomi Ito for technical support and Dr. Jennifer Logan for help with editing the manuscript.

REFERENCES

1. Barresi, R., and Campbell, K. P. (2006) *J. Cell. Sci.* **119,** 199–207
2. Cohn, R. D., Henry, M. D., Michele, D. E., Barresi, R., Saito, F., Moore, S. A., Flanagan, J. D., Skwarchuk, M. W., Robbins, M. E., Mendell, J. R., Williamson, R. A., and Campbell, K. P. (2002) *Cell* **110,** 639–648
3. Han, R., Kanagawa, M., Yoshida-Moriguchi, T., Rader, E. P., Ng, R. A., Michele, D. E., Muirhead, D. E., Kunz, S., Moore, S. A., Iannaccone, S. T., Miyake, K., McNeil, P. L., Mayer, U., Oldstone, M. B., Faulkner, J. A., and Campbell, K. P. (2009) *Proc. Natl. Acad. Sci. U.S.A.* **106,** 12573–12579
4. Michele, D. E., Kabaeva, Z., Davis, S. L., Weiss, R. M., and Campbell, K. P. (2009) *Circ. Res.* **105,** 984–993
5. Moore, S. A., Saito, F., Chen, J., Michele, D. E., Henry, M. D., Messing, A., Cohn, R. D., Ross-Barta, S. E., Westra, S., Williamson, R. A., Hoshi, T., and Campbell, K. P. (2002) *Nature* **418,** 422–425
6. Saito, F., Moore, S. A., Barresi, R., Henry, M. D., Messing, A., Ross-Barta, S. E., Cohn, R. D., Williamson, R. A., Sluka, K. A., Sherman, D. L., Brophy, P. J., Schmelzer, J. D., Low, P. A., Wrabetz, L., Feltri, M. L., and Campbell, K. P. (2003) *Neuron* **38,** 747–758
7. Satz, J. S., Philp, A. R., Nguyen, H., Kusano, H., Lee, J., Turk, R., Riker, M. J., Hernández, J., Weiss, R. M., Anderson, M. G., Mullins, R. F., Moore, S. A., Stone, E. M., and Campbell, K. P. (2009) *J. Neurosci.* **29,** 13136–13146
8. Chiba, A., Matsumura, K., Yamada, H., Inazu, T., Shimizu, T., Kusunoki, S., Kanazawa, I., Kobata, A., and Endo, T. (1997) *J. Biol. Chem.* **272,** 2156–2162
9. Manya, H., Chiba, A., Yoshida, A., Wang, X., Chiba, Y., Jigami, Y., Margolis, R. U., and Endo, T. (2004) *Proc. Natl. Acad. Sci. U.S.A.* **101,** 500–505
10. Beltrán-Valero de Bernabé, D., Currier, S., Steinbrecher, A., Celli, J., van Beusekom, E., van der Zwaag, B., Kayserili, H., Merlini, L., Chitayat, D., Dobyns, W. B., Cormand, B., Lehesjoki, A. E., Cruces, J., Voit, T., Walsh, C. A., van Bokhoven, H., and Brunner, H. G. (2002) *Am. J. Hum. Genet.* **71,** 1033–1043
11. van Reeuwijk, J., Janssen, M., van den Elzen, C., Beltran-Valero de Bernabé, D., Sabatelli, P., Merlini, L., Boon, M., Scheffer, H., Brockington, M., Muntoni, F., Huynen, M. A., Verrips, A., Walsh, C. A., Barth, P. G., Brunner, H. G., and van Bokhoven, H. (2005) *J. Med. Genet.* **42,** 907–912
12. Yoshida, A., Kobayashi, K., Manya, H., Taniguchi, K., Kano, H., Mizuno, M., Inazu, T., Mitsuhashi, H., Takahashi, S., Takeuchi, M., Herrmann, R., Straub, V., Talim, B., Voit, T., Topaloglu, H., Toda, T., and Endo, T. (2001) *Dev. Cell* **1,** 717–724
13. Yoshida-Moriguchi, T., Yu, L., Stalnaker, S. H., Davis, S., Kunz, S., Madson, M., Oldstone, M. B., Schachter, H., Wells, L., and Campbell, K. P. (2010) *Science* **327,** 88–92
14. Kobayashi, K., Nakahori, Y., Miyake, M., Matsumura, K., Kondo-Iida, E., Nomura, Y., Segawa, M., Yoshioka, M., Saito, K., Osawa, M., Hamano, K., Sakakihara, Y., Nonaka, I., Nakagome, Y., Kanazawa, I., Nakamura, Y., Tokunaga, K., and Toda, T. (1998) *Nature* **394,** 388–392
15. Brockington, M., Blake, D. J., Prandini, P., Brown, S. C., Torelli, S., Benson, M. A., Ponting, C. P., Estournet, B., Romero, N. B., Mercuri, E., Voit, T., Sewry, C. A., Guicheney, P., and Muntoni, F. (2001) *Am. J. Hum. Genet.* **69,** 1198–1209
16. Grewal, P. K., Holzfeind, P. J., Bittner, R. E., and Hewitt, J. E. (2001) *Nat. Genet.* **28,** 151–154
17. Barresi, R., Michele, D. E., Kanagawa, M., Harper, H. A., Dovico, S. A., Satz, J. S., Moore, S. A., Zhang, W., Schachter, H., Dumanski, J. P., Cohn, R. D., Nishino, I., and Campbell, K. P. (2004) *Nat. Med.* **10,** 696–703
18. Muntoni, F., Torelli, S., and Brockington, M. (2008) *Neurotherapeutics* **5,** 627–632
19. Godfrey, C., Clement, E., Mein, R., Brockington, M., Smith, J., Talim, B., Straub, V., Robb, S., Quinlivan, R., Feng, L., Jimenez-Mallebrera, C., Mercuri, E., Manzur, A. Y., Kinali, M., Torelli, S., Brown, S. C., Sewry, C. A., Bushby, K., Topaloglu, H., North, K., Abbs, S., and Muntoni, F. (2007) *Brain* **130,** 2725–2735
20. Lisi, M. T., and Cohn, R. D. (2007) *Biochim. Biophys. Acta* **1772,** 159–172
21. Sigesmund, D. A., Weleber, R. G., Pillers, D. A., Westall, C. A., Panton, C. M., Powell, B. R., Héon, E., Murphey, W. H., Musarella, M. A., and Ray, P. N. (1994) *Ophthalmology* **101,** 856–865
22. Sato, S., Omori, Y., Katoh, K., Kondo, M., Kanagawa, M., Miyata, K., Funabiki, K., Koyasu, T., Kajimura, N., Miyoshi, T., Sawai, H., Kobayashi, K., Tani, A., Toda, T., Usukura, J., Tano, Y., Fujikado, T., and Furukawa, T. (2008) *Nat. Neurosci.* **11,** 923–931
23. Lee, Y., Kameya, S., Cox, G. A., Hsu, J., Hicks, W., Maddatu, T. P., Smith, R. S., Naggert, J. K., Peachey, N. S., and Nishina, P. M. (2005) *Mol. Cell. Neurosci.* **30,** 160–172
24. Liu, J., Ball, S. L., Yang, Y., Mei, P., Zhang, L., Shi, H., Kaminski, H. J., Lemmon, V. P., and Hu, H. (2006) *Mech. Dev.* **123,** 228–240
25. Kanagawa, M., Nishimoto, A., Chiyonobu, T., Takeda, S., Miyagoe-Suzuki, Y., Wang, F., Fujikake, N., Taniguchi, M., Lu, Z., Tachikawa, M., Nagai, Y., Tashiro, F., Miyazaki, J., Tajima, Y., Takeda, S., Endo, T., Kobayashi, K., Campbell, K. P., and Toda, T. (2009) *Hum. Mol. Genet.* **18,** 621–631
26. Miyagoe-Suzuki, Y., Masubuchi, N., Miyamoto, K., Wada, M. R., Yuasa, S., Saito, F., Matsumura, K., Kanesaki, H., Kudo, A., Manya, H., Endo, T., and Takeda, S. (2009) *Mech. Dev.* **126,** 107–116
27. Ervasti, J. M., and Campbell, K. P. (1993) *J. Cell Biol.* **122,** 809–823
28. Gee, S. H., Montanaro, F., Lindenbaum, M. H., and Carbonetto, S. (1994) *Cell* **77,** 675–686
29. Ervasti, J. M., Burwell, A. L., and Geissler, A. L. (1997) *J. Biol. Chem.* **272,** 22315–22321
30. Kanagawa, M., Saito, F., Kunz, S., Yoshida-Moriguchi, T., Barresi, R., Kobayashi, Y. M., Muschler, J., Dumanski, J. P., Michele, D. E., Oldstone, M. B., and Campbell, K. P. (2004) *Cell* **117,** 953–964
31. Sugita, S., Saito, F., Tang, J., Satz, J., Campbell, K., and Südhof, T. C. (2001)

J. Cell Biol. **154,** 435–445
32. Hohenester, E., Tisi, D., Talts, J. F., and Timpl, R. (1999) *Mol. Cell* **4,** 783–792
33. Talts, J. F., Andac, Z., Göhring, W., Brancaccio, A., and Timpl, R. (1999) *EMBO J.* **18,** 863–870
34. Bao, X., Kobayashi, M., Hatakeyama, S., Angata, K., Gullberg, D., Nakayama, J., Fukuda, M. N., and Fukuda, M. (2009) *Proc. Natl. Acad. Sci. U.S.A.* **106,** 12109–12114
35. Holzfeind, P. J., Grewal, P. K., Reitsamer, H. A., Kechvar, J., Lassmann, H., Hoeger, H., Hewitt, J. E., and Bittner, R. E. (2002) *Hum. Mol. Genet.* **11,** 2673–2687
36. Montanaro, F., Carbonetto, S., Campbell, K. P., and Lindenbaum, M. (1995) *J. Neurosci. Res.* **42,** 528–538
37. Blank, M., Koulen, P., and Kröger, S. (1997) *J. Comp. Neurol.* **389,** 668–678
38. Koulen, P., Blank, M., and Kröger, S. (1998) *J. Neurosci. Res.* **51,** 735–747
39. Blank, M., Koulen, P., Blake, D. J., and Kröger, S. (1999) *Eur. J. Neurosci.* **11,** 2121–2133
40. Jastrow, H., Koulen, P., Altrock, W. D., and Kröger, S. (2006) *Invest. Ophthalmol. Vis. Sci.* **47,** 17–24
41. Ohlendieck, K., and Campbell, K. P. (1991) *J. Cell. Biol.* **115,** 1685–1694
42. Cibis, G. W., Fitzgerald, K. M., Harris, D. J., Rothberg, P. G., and Rupani, M. (1993) *Invest. Ophthalmol. Vis. Sci.* **34,** 3646–3652
43. Pillers, D. A., Fitzgerald, K. M., Duncan, N. M., Rash, S. M., White, R. A., Dwinnell, S. J., Powell, B. R., Schnur, R. E., Ray, P. N., Cibis, G. W., and Weleber, R. G. (1999) *Hum. Genet.* **105,** 2–9
44. D'Souza, V. N., Nguyen, T. M., Morris, G. E., Karges, W., Pillers, D. A., and Ray, P. N. (1995) *Hum. Mol. Genet.* **4,** 837–842
45. Kameya, S., Araki, E., Katsuki, M., Mizota, A., Adachi, E., Nakahara, K., Nonaka, I., Sakuragi, S., Takeda, S., and Nabeshima, Y. (1997) *Hum. Mol. Genet.* **6,** 2195–2203

Defective glycosylation of α-dystroglycan contributes to podocyte flattening

Kenichiro Kojima[1], Hitonari Nosaka[1], Yuki Kishimoto[1], Yuri Nishiyama[1], Seiichi Fukuda[1], Masaru Shimada[1], Kenzo Kodaka[1], Fumiaki Saito[2], Kiichiro Matsumura[2], Teruo Shimizu[2], Tatsushi Toda[3], Satoshi Takeda[4], Hiroshi Kawachi[5] and Shunya Uchida[1]

[1]Department of Internal Medicine, Teikyo University School of Medicine, Tokyo, Japan; [2]Department of Neurology and Neuroscience, Teikyo University School of Medicine, Tokyo, Japan; [3]Division of Clinical Genetics, Department of Medical Genetics, Osaka University Graduate School of Medicine, Osaka, Japan; [4]Otsuka GEN Research Institute, Otsuka Pharmaceutical, Tokushima, Japan and [5]Institute of Nephrology, Niigata University, Niigata, Japan

In addition to skeletal muscle and the nervous system, α-dystroglycan is found in the podocyte basal membrane, stabilizing these cells on the glomerular basement membrane. Fukutin, named after the gene responsible for Fukuyama-type congenital muscular dystrophy, is a putative glycosyltransferase required for the post-translational modification of α-dystroglycan. Chimeric mice targeted for both alleles of *fukutin* develop severe muscular dystrophy; however, these mice do not have proteinuria. Despite the lack of a functional renal defect, we evaluated glomerular structure and found minor abnormalities in the chimeric mice by light microscopy. Electron microscopy revealed flattening of podocyte foot processes, the number of which was significantly lower in the chimeric compared to wild-type mice. A monoclonal antibody against the laminin-binding carbohydrate residues of α-dystroglycan did not detect α-dystroglycan glycosylation in the glomeruli by immunoblotting or immunohistochemistry. In contrast, expression of the core α-dystroglycan protein was preserved. There was no statistical difference in dystroglycan mRNA expression or in the amount of nephrin and α3-integrin protein in the chimeric compared to the wild-type mice as judged by immunohistochemistry and real-time RT-PCR. Thus, our results indicate that appropriate glycosylation of α-dystroglycan has an important role in the maintenance of podocyte architecture.

Kidney International (2011) **79,** 311–316; doi:10.1038/ki.2010.403; published online 13 October 2010

KEYWORDS: adhesion molecule; dystroglycan; foot process; glycosylation; podocyte

Correspondence: *Kenichiro Kojima, Department of Internal Medicine, Teikyo University School of Medicine, 2-11-1 Kaga, Itabashi-ku, Tokyo 173-8605, Japan. E-mail: kojima@med.teikyo-u.ac.jp*

Received 26 January 2010; revised 12 August 2010; accepted 31 August 2010; published online 13 October 2010

Podocytes are highly differentiated cells that possess specialized projections called foot processes. Adhesion molecules of podocytes are likely to have an important role in the maintenance of podocyte morphology by anchoring of these cells to the glomerular basement membrane (GBM).[1,2] To date, two major adhesion protein systems have been identified. As the first step, $\alpha_3\beta_1$-integrin was localized exclusively to the podocyte basal membrane domains in normal and flattened human podocytes and was speculated to contribute to the firm adhesion of the podocytes to the GBM matrix proteins.[3–5]

Recently, α- and β-dystroglycans were discovered in podocytes, and were found to be localized to the podocytes basal membrane domain.[6,7] Dystroglycan is composed of a transmembrane, heterodimeric complex of α- and β-subunits that link the extracellular matrix to the cell cytoskeleton. Gene knockout experiments have not been helpful for understanding the role of dystroglycans in podocyte function, because knockout results in early embryonic death, long before kidney glomeruli develop, and because Reichert's membrane, the first canonical basement membrane produced by the embryo, is disorganized, and it fails to withstand the blood pressure of maternal circulation.[8]

Fukuyama-type congenital muscular dystrophy (FCMD), discovered in Japan, is a severe muscular dystrophy with central nervous system involvement.[9] Fukutin, named after the gene responsible for FCMD, is a putative glycosyltransferase required for post-translational modification of α-dystroglycan.[10,11]

Chimeric mice generated using embryonic stem cells targeted for both *fukutin* alleles develop severe muscular dystrophy associated with the defective glycosylation of α-dystroglycan.[12] In this study, we investigated fukutin-deficient chimeric mice to clarify the role of α-dystroglycan glycosylation for maintaining podocyte architecture.

RESULTS

Chimeric mice showed muscle weakness, were unable to walk in a straight line, and dragged their feet as previously described.[12]

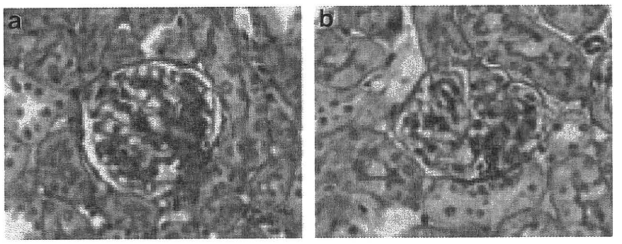

Figure 1 | Photomicrographs of periodic acid Schiff stain. Representative photomicrographs of wild-type (**a**) and the fukutin-deficient chimeric mice (**b**). Glomeruli from the fukutin-deficient chimeric mice have no abnormalities by light microscopy. Original magnification × 200.

Figure 2 | Transmitted electron photomicrograph of the fukutin-deficient chimeric mice. The flattening of foot processes was observed in segmental lesion of capillary lumens (arrowheads). No detachment of foot processes from the GBM was observed. Original magnification × 4000. GBM, glomerular basement membrane.

Light microscopy of kidney specimens showed minor abnormalities (Figure 1) together without massive albuminuria. Electron microscopy revealed morphological changes in podocytes such as vacuolization, microvillous transformation, and segmental foot process effacement. However, the detachment of foot processes from the GBM was not observed (Figure 2). The number of foot processes along the GBM decreased significantly in chimeric mice (1.39 ± 0.18/ μm GBM; Figure 3b) compared with wild-type mice (2.09 ± 0.01/μm GBM; Figure 3a) ($P = 0.039$; Figure 3c). In addition, the GBM was thickened and the three-layered structure of the GBM was lost under the lesion of flattened foot processes in chimeric mice (Figure 3b). The thickness of the GBM was increased significantly in chimeric mice (0.30 ± 0.03 μm) compared with wild-type mice (0.15 ± 0.01 μm) ($P = 0.043$; Figure 3d).

Immunohistochemistry using the IIH6 monoclonal antibody against the laminin-binding carbohydrate residues of α-dystroglycan (Figure 4a) and rabbit polyclonal antibody AP1530 against the 34 amino acids in the C-terminal domain of human α-dystroglycan indicated that the α-dystroglycan was localized along the glomerular capillary walls in a linear manner in wild-type mice kidneys (Figure 4c). In contrast, the expression of α-dystroglycan laminin-binding carbohydrate residues decreased in chimeric mice (Figure 4b). Immunohistochemistry revealed that expression of the core α-dystroglycan protein was relatively preserved in chimeric mice (Figure 4d).

In wild-type mice, immunoblotting detected a broad band around 150 kDa representing α-dystroglycan (Figure 4e). Expression of laminin-binding carbohydrate residues was reduced in chimeric mice (Figure 4e), whereas that of the core α-dystroglycan protein was relatively preserved in chimeric mice. An additional band around 75 kDa was detected in chimeric mice, suggesting that considerable parts of α-dystroglycan were hypoglycosylated (Figure 4f). There was no statistical difference in the mRNA expression of dystroglycan between the wild-type and chimeric mice (Figure 4g).

In wild-type mice, a laminin overlay assay detected a broad band around 150 kDa corresponding to α-dystroglycan, whereas the overlay assay revealed a deficiency in the laminin-binding activity of α-dystroglycan in chimeric mice (Figure 4h).

The expression of α_3-integrin (another adhesion molecule localized to the podocytes basal membrane domain) and nephrin (which is thought to be the main component of the slit diaphragm)[13] was also investigated. The expression levels of α_3-integrin and nephrin were unaltered in chimeric mice using immunohistochemistry and real-time RT-PCR (Figure 5a–d, g, and h).

Tetramethylrhodamine (TRITC)-conjugated wheat germ agglutinin (WGA) staining was performed to detect sialic acid and *N*-acetyl-glucosamine (GlcNAc) oligomer. WGA staining was observed along the glomerular capillary walls in a linear manner in wild-type mice. Similar staining was observed in chimeric mice, suggesting that fukutin deficiency did not affect GlcNAc oligomers and sialic acid (Figure 5e and f).

DISCUSSION

Dystroglycan is expressed in many cell types such as skeletal muscles, various epithelia, and in the nervous system.[14,15] α-Dystroglycan is heavily glycosylated by *O*-mannosyl glycosylation. It is speculated that α-dystroglycan carbohydrate residues are bound to the cationic LG domain common to several matrix proteins such as laminin and agrin.[16] In the glomerulus, α-dystroglycan is localized to basal cell membrane domains of the podocyte, stabilizes podocytes on the GBM, and presumably is involved in the pathogenesis of foot process flattening.[17]

Using the IIH6 monoclonal antibody, we found that the expression of α-dystroglycan laminin-binding carbohydrate residues decreased in fukutin-deficient chimeric mice, whereas expression of the core α-dystroglycan protein was preserved. These results confirmed that fukutin is involved in the modification of α-dystroglycan laminin-binding carbohydrate residues. We performed the laminin blot overlay assay to evaluate the binding activity of α-dystroglycan to laminin and revealed a severe reduction in the binding

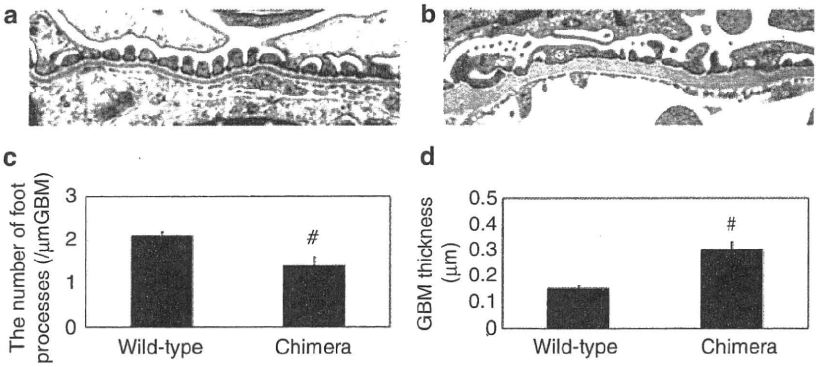

Figure 3 | The number of foot processes and the thickness of the GBM. Representative transmitted electron photomicrographs of wild-type (**a**) and the fukutin-deficient chimeric mice (**b**). The GBM under the foot process effacement is thickened and the three-layered structure is lost. The number of foot processes per μm GBM (**c**) and the thickness of the GBM (**d**) in wild-type mice (wild-type) and the chimeric mice (chimera). Values are expressed as means ± s.d. $^{\#}P<0.05$ vs wild type. GBM, glomerular basement membrane.

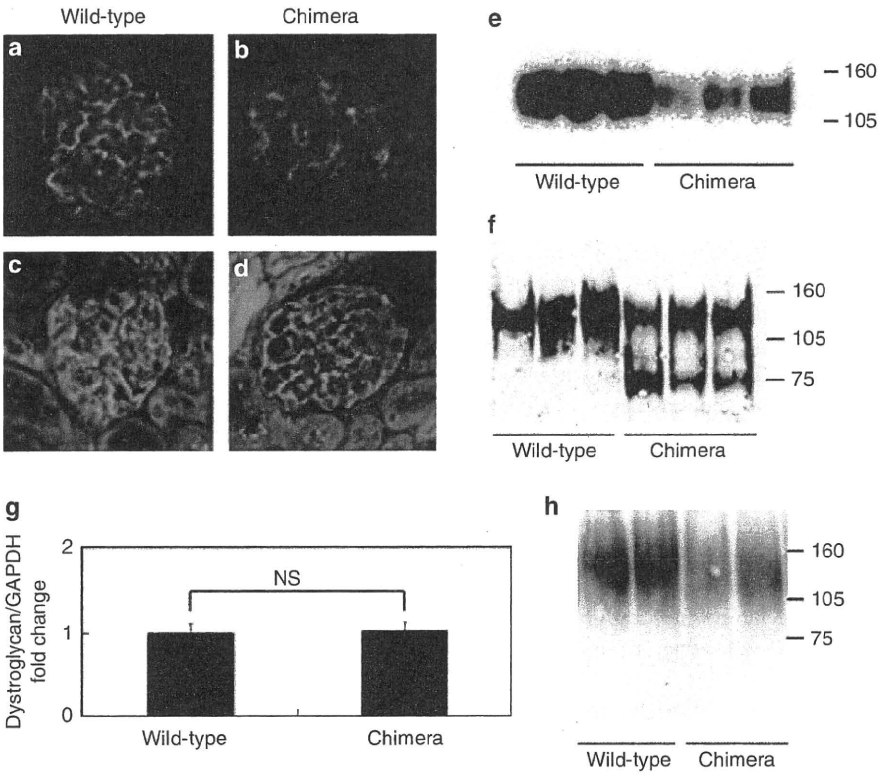

Figure 4 | Defective glycosylation of α-dystroglycan decreases the binding activity to laminin. Immunohistochemistry (**a–d**) and immunoblotting (**e**, **f**) reveal reduction of the laminin-binding carbohydrate residues of α-dystroglycan (**a**, **b**, **e**) in the chimeric mice (chimera) compared with the wild-type mice (wild-type). Expression of core protein of α-dystroglycan (**c**, **d**, **f**) is relatively preserved in the chimeric mice (chimera). The additional band around 75 kDa is detected in the chimeric mice, suggesting considerable parts of α-dystroglycan are hypoglycosylated (**f**). (**g**) Expression of dystroglycan by real-time RT-PCR in the wild-type mice (wild-type) and the chimeric mice (chimera). (**h**) Laminin binding activity of α-dystroglycan. Blot overlay analysis shows that the binding activity of α-dystroglycan is decreased in the chimeric mice (chimera). NS, not significant

activity in chimeric mice. Previously we reported that injury to α-dystroglycan with reactive oxygen species or protamine sulfate directly split the attachments of α-dystroglycan to laminin and agrin, and this led to the induction of foot process flattening.[17] Similar results were also found that for deglycosylated α-dystroglycan by reactive oxygen species, which led to impaired binding to laminin and agrin, and to foot process flattening.[18] These data suggest that defective glycosylation of α-dystroglycan causes inhibition of binding to laminin and agrin resulting in the flattening of foot processes.

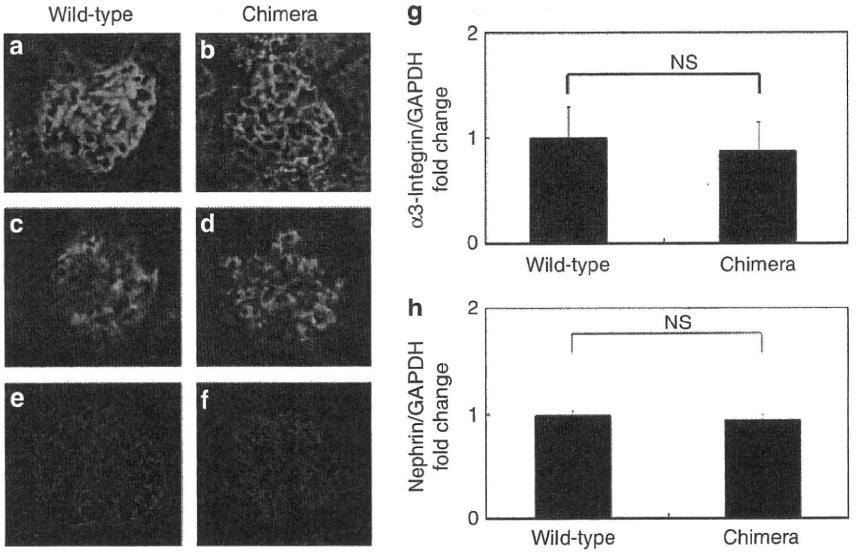

Figure 5 | Expression of α_3-integrin or nephrin, and WGA lectin staining. Immunohistochemistry (**a**–**d**) and real-time RT-PCR (**g**, **h**) for α_3-integrin (**a**, **b**, **g**) or nephrin (**c**, **d**, **h**), and TRITC-conjugated WGA lectin staining (**e**, **f**) in the wild-type mice (wild-type) or the chimeric mice (chimera). Expressions of α_3-integrin and nephrin are preserved in the chimeric mice (**b**, **d**). WGA staining is localized along the glomerular capillary walls in wild-type (**e**) and chimera (**f**). NS, not significant; TRITC, tetramethylrhodamine; WGA, wheat germ agglutinin.

The podocyte structure was changed in the fukutin-deficient chimeric mice. However, there was no detachment of foot processes from the GBM. The expression of α_3-integrin (another adhesion molecule localized to the podocyte basal membrane domain) was preserved in chimeric mice. Kitsiou *et al.*[19] found that anti-α_3-integrin monoclonal antibody decreased the adhesion of human podocytes to collagen type IV. Homozygous mutant mice with targeted knockout of α_3-integrin fail to form complete foot processes resulting in podocyte detachment.[20] The presence of α_3-integrin in chimeric mice might rescue the detachment of podocytes from the GBM.

WGA lectin staining was performed to detect sialic acid and GlcNAc oligomer in the glomerular capillaries. Sialic acid residues on podocalyxin and other glycoproteins are essential for maintenance of podocyte architecture.[21,22] Defect of heparan sulfate glycosaminoglycan containing GlcNAc oligomer is shown to induce foot process effacement without severe proteinuria.[23] WGA staining was retained in chimeric mice, suggesting that fukutin deficiency was not affecting glycosylation of other glycoproteins except for α-dystroglycan.

It is interesting to note that urinary protein excretion did not increase in chimeric mice despite the flattening of foot processes. One reason for this phenomenon may be that the degree of foot process effacement was not extensive. Furthermore, the expressions of α_3-integrin and nephrin were relatively preserved in chimeric mice. We reported decreased α_3-integrin expression and foot process effacement, which precedes the development of proteinuria, in puromycin aminonucleoside nephrosis.[5] In this study, the retained α_3-integrin might contribute to the prevention of proteinuria in chimeric mice. Nephrin, a member of the Ig superfamily, was first discovered as one of the slit diaphragm proteins.[13] Mutations in nephrin lead to a loss of normal podocyte structure, resulting in fetal proteinuria in congenital nephrotic syndrome of the Finnish type.[24,25] Some investigators have reported that nephrin expression is lower in patients with primary acquired nephrotic syndrome.[26,27] In this study, preserved α_3-integrin and nephrin might have prevented proteinuria in chimeric mice.

So far, no information is available concerning glomerular changes in FCMD in the literature, because these patients usually do not develop proteinuria. Most patients with FCMD develop serious muscle weakness, global developmental delay, and die by 20 years of age.[9] The lack of long-term survival might disturb development of proteinuria in FCMD patients. However, the possibility that foot process effacement occurs subtly in these patients during their infantile periods cannot be ruled out.

A generalized gene knockout of dystroglycan results in early embryonic death before the development of renal glomeruli[8] because the Reichiert's membrane matrix proteins are disorganized. Fukutin homozygous-null mice also cannot survive beyond an early embryonic stage because of the fragility of the basement membranes.[28] An example of dystroglycan function is observed in skeletal muscle cells where it mediates the redistribution of matrix proteins under the control of the actin cytoskeleton, and *vice versa*.[29] High-resolution electron microscopy showed that arrays of fibers in the lamina rara externa are irregularly arranged in puromycin aminonucleoside nephrosis and after protamine sulfate

perfusion.[17] Similar to that study, this study showed that chimeric mice had a significant increase in the thickness of the GBM with a loss of its three-layered structure. These findings imply that α-dystroglycan is important for organizing extracellular matrix proteins and forming a stable basement membrane structure in the glomerulus.

In conclusion, the results of this study indicate that appropriate glycosylation of α-dystroglycan may be important in the maintenance of podocyte architecture and matrix assembly in the GBM. Further investigation into the relationships of slit membrane-related molecules, cytoskeletal proteins, and adhesion molecules is essential to clarify the mechanisms of proteinuria.

MATERIALS AND METHODS

Antibodies and lectin

Mouse monoclonal antibodies against laminin-binding carbohydrate residues of α-dystroglycan (IIH6) were obtained from Upstate Biotechnology (Lake Placid, NY). Rabbit anti-laminin antibody was purchased from Sigma Chemical (St Louis, MO). Rabbit anti-human α_3-integrin polyclonal antiserum was obtained from Chemicon International (Temecula, CA). Preparations of rabbit polyclonal antibody against the 34 amino acids in the C-terminal domain of human α-dystroglycan (AP1530) and anti-nephrin antibody were described previously.[30,31] fluorescein isothiocyanate- or horseradish peroxidase-conjugated secondary antibodies were obtained from Dako (Glostrup, Denmark). TRITC-conjugated WGA was obtained from Vector Laboratories (Burlingame, PA).

Animals

Fukutin-deficient chimeric mice were generated using embryonic stem cells targeted for both *fukutin* alleles ($n=3$) as previously reported.[12] C57BL/6 mice were used as normal controls ($n=3$). Mice were killed at 7 months of age. All animal experiments were approved by the local ethics committee.

Urinary albumin excretion was determined using Albustix (Bayer Medical, Tokyo, Japan).

Light microscopy, immunochemistry, and lectin histochemistry

Renal cortices were fixed in 4% paraformaldehyde, embedded in paraffin, and 4 μm-thick sections were cut. Sections were stained with Periodic acid-Schiff reaction.

Frozen sections (4-μm thick) were cut and stained using the indirect immunofluorescence method. TRITC-conjugated WGA staining was performed according to the manufacturer's instructions.

Electron microscopy

The fixed renal cortices were embedded in epoxy resin using conventional methods. Ultrathin sections were prepared, stained with uranyl acetate and lead citrate, and were then examined with a JEOL 1200EX electron microscope (JEOL, Tokyo, Japan). To evaluate the morphological changes in podocytes, the number of epithelial foot processes per μm of GBM and thickness of GBM were calculated using a curvimeter. Three glomeruli were randomly selected from each mouse and 10 electron micrographs were taken in each glomerulus. Areas of wrinkled GBM were excluded. The measurements were taken from electron micrographs with magnifications of × 10,000.

Immunoblotting

Mouse kidney cortices were extracted with RIPA buffer (20 mM Tris-HCl, 150 mM NaCl, 2 mM EDTA, 1% Nonidet P-40, 1% sodium deoxycholate, 0.1% SDS) for 2 h at 4 °C, followed by centrifugation at 500 *g* for 5 min. The supernatants were dissolved in SDS sample buffer and electrophoresed on 7.5% polyacrylamide gels under reducing conditions. Gels loaded with samples were transferred onto nitrocellulose membranes (Amersham Pharmacia Biotech, Uppsala, Sweden). Immunoblotting was performed with the primary antibodies, and detection was performed with an enhanced chemiluminescence kit (Amersham Pharmacia Biotech).

Blot overlay analysis

The nitrocellulose transfers of renal cortex lysates were blocked in 10 mM Tris-HCl (pH 7.6), 140 mM NaCl, 1 mM $CaCl_2$, and 1 mM $MgCl_2$ (LBB) containing 5% non-fat dry milk for 1 h at room temperature. The transfers were incubated with LBB containing 0.1–0.5 μg per stripe EHS laminin (Koken, Tokyo, Japan) overnight at 4 °C. Bound laminin was detected using anti-laminin antibody and the development was conducted with an enhanced chemiluminescence kit (Amersham).

Real-time RT-PCR

RNA was isolated from renal tissues using TRIzol reagent (Invitrogen, Paisley, UK) according to the manufacturer's instructions. Total RNA (1 μg) was used as a template. Real-time RT-PCR was performed using the LightCycler FastStart kit with SYBR Green (Roche Molecular Systems, Alameda, CA). Reaction conditions were as follows: an initial hold at 50 °C for 10 min followed by 95 °C for 5 min to achieve first-strand synthesis. PCR was cycled for 40 iterations; 95 °C for 10 s, 55 °C for 30 s, and 72 °C for 1 min. The Reaction was completed at 72 °C for 10 min. The primer pairs used were: $\alpha_3\beta_1$-integrin (forward, TCCGTGGACATCGACTCTGA; reverse, AGCTTCATACAGGGCACGAG), dystroglycan (forward, GGACCCTGAGAAGAGCAGTG; reverse, TGGTAGGGAGGTGCATTAGG), nephrin (forward, GATCCAGGTCTCCGTCACTA; reverse, GAAGACCACCAACTGCAAAG). The transcript level in the wild-type was arbitrarily expressed as 1.

Statistics

All data are expressed as means ± s.d. Values were analyzed by unpaired Student's *t*-test. $P<0.05$ was considered significant.

DISCLOSURE

All the authors declared no competing interests.

REFERENCES

1. Kerjaschki D. Caught flat-footed: podocyte damage and the molecular bases of focal glomerulosclerosis. *J Clin Invest* 2001; **108**: 1583–1587.
2. Durvasula RV, Shankland SJ. Podocyte injury and targeting therapy: an update. *Curr Opin Nephrol Hypertens* 2006; **15**: 1–7.
3. Kerjaschki D, Ojha PP, Susani M *et al.* A β1-integrin receptor for fibronectin in human glomeruli. *Am J Pathol* 1989; **134**: 481–489.
4. Adler S. Characterization of glomerular epithelial cell matrix receptors. *Am J Pathol* 1992; **141**: 571–578.
5. Kojima K, Matsui K, Nagase M. Protection of α3 integrin-mediated podocyte shape by superoxide dismutase in the puromycin aminonucleoside nephrosis rat. *Am J Kidney Dis* 2000; **35**: 1175–1185.
6. Regele HM, Fillipovic E, Langer B *et al.* Glomerular expression of dystroglycans is reduced in minimal change nephrosis but not in focal segmental glomerulosclerosis. *J Am Soc Nephrol* 2000; **11**: 403–412.
7. Raats CJ, van Den Born J, Bakker MA *et al.* Expression of agrin, dystroglycan, and utrophin in normal renal tissue and in experimental glomerulopathies. *Am J Pathol* 2000; **156**: 1749–1765.

8. Williamson RA, Henry MD, Daniels KJ *et al.* Dystroglycan is essential for early embryonic development: disruption of Reichert's membrane in *Dag1*-null mice. *Hum Mol Genet* 1997; **6**: 831–841.
9. Fukuyama Y, Osawa M, Suzuki H. Congenital progressive muscular dystrophy of the Fukuyama type-clinical, genetic, and pathological considerations. *Brain Dev* 1981; **3**: 1–29.
10. Toda T, Segawa M, Nomura Y *et al.* Localization of a gene for Fukuyama type congenital muscular dystrophy to chromosome 9q31-33. *Nat Genet* 1993; **5**: 283–286.
11. Toda T, Miyake M, Kobayashi K *et al.* Linkage-disequilibrium mapping narrows the Fukuyama-type congenital muscular dystrophy (FCMD) candidate region to <100 kb. *Am J Hum Genet* 1996; **59**: 1313–1320.
12. Takeda S, Kondo M, Sasaki J *et al.* Fukutin is required for maintenance of muscle integrity, cortical histiogenesis and normal eye development. *Hum Mol Genet* 2003; **12**: 1449–1459.
13. Ruotsalainen V, Ljungberg P, Wartiovaara J *et al.* Nephrin is specifically located at the slit diaphragm of glomerular podocytes. *Proc Natl Acad Sci USA* 1999; **96**: 7962–7967.
14. Hemler ME. Dystroglycan versatility. *Cell* 1999; **97**: 543–546.
15. Durbeej M, Henry MD, Campbell KP. Dystroglycan in development and disease. *Curr Opin Cell Biol* 1998; **10**: 594–601.
16. Hohenester E, Tisi D, Talts JF *et al.* The crystal structure of a laminin G-like module reveals the molecular basis of alpha-dystroglycan binding to laminins, perlecan, and agrin. *Mol Cell* 1999; **4**: 783–792.
17. Kojima K, Davidovits A, Poczewski H *et al.* Podocyte flattening and disorder of glomerular basement membrane are associated with splitting of dystroglycan-matrix interaction. *J Am Soc Nephrol* 2004; **15**: 2079–2089.
18. Vogtländer NPJ, Tamboer WPM, Bakker MAH *et al.* Reactive oxygen species deglycosilate glomerular α-dystroglycan. *Kidney Int* 2006; **69**: 1526–1534.
19. Kitsiou PV, Tzinia AK, Stetler-Sterenson WG *et al.* Glucose-induced changes in integrins and matrix-related function in cultured human glomerular epithelial cells. *Am J Physiol* 2003; **285**: F40–F48.
20. Kreidberg JA, Donovan MJ, Goldstein SL *et al.* Alpha 3 beta 1 integrin has a crucial role in kidney and lung organogenesis. *Development* 1996; **122**: 3537–3547.
21. Andrews PM. Glomerular epithelial alterations resulting from sialic acid surface coat removal. *Kidney Int* 1979; **15**: 376–385.
22. Galeano B, Klootwijk R, Manoli I *et al.* Mutation in the key enzyme of sialic acid biosynthesis causes severe glomerular proteinuria and is rescued by *N*-acetylmannosamine. *J Clin Invest* 2007; **117**: 1585–1594.
23. Chen S, Wassenhove-McCarthy DJ, Yamaguchi Y *et al.* Loss of heparan sulfate glycosaminoglycan assembly in podocytes does not lead proteinuria. *Kidney Int* 2008; **74**: 289–299.
24. Kestila M, Ienkkeri U, Mannikko M *et al.* Positionally cloned gene for a novel glomerular protein—nephrin—is mutated in congenital nephrotic syndrome. *Mol Cell* 1998; **1**: 575–582.
25. Tryggvason K, Ruotsalainen V, Wartiovaara J. Discovery of the congenital nephrotic syndrome gene discloses the structure of the mysterious molecular sieve of the kidney. *Int J Dev Biol* 1999; **43**: 445–451.
26. Doublier S, Routsalainen V, Salvidio G *et al.* Nephrin redistribution on podocytes is a potential mechanism for proteinuria in patients with primary acquired nephrotic syndrome. *Am J Pathol* 2001; **158**: 1723–1731.
27. Wernerson A, Duner F, Pettersson E *et al.* Altered ultrastructural distribution of nephrin in minimal change nephrotic syndrome. *Nephrol Dial Transplant* 2003; **18**: 70–76.
28. Kurahashi H, Taniguchi M, Meno C *et al.* Basement membrane fragility underlies embryonic lethality in *fukutin*-null mice. *Neurobiol Dis* 2005; **19**: 208–217.
29. Colognato H, Winkelmann DA, Yurchenco PD. Laminin polymerization induces a receptor-cytoskeleton network. *J Cell Biol* 1999; **145**: 619–631.
30. Saito F, Masaki T, Saito Y *et al.* Defective peripheral nerve myelination and neuromuscular junction formation in fukutin-deficient chimeric mice. *J Neurochem* 2007; **101**: 1712–1722.
31. Kawachi H, Koike H, Kurihara H *et al.* Cloning of rat nephrin: expression in developing glomeruli and in proteinuric states. *Kidney Int* 2000; **57**: 1949–1961.

Glycobiology vol. 20 no. 9 pp. 1089–1102, 2010
doi:10.1093/glycob/cwq069
Advance Access publication on May 10, 2010

Protein *O*-mannosylation is necessary for normal embryonic development in zebrafish

Eriko Avşar-Ban[2,*], Hisayoshi Ishikawa[2,*], Hiroshi Manya[3], Masatoki Watanabe[2], Shinichi Akiyama[2,5], Hideo Miyake[2,4], Tamao Endo[3], and Yutaka Tamaru[1,2,4]

[2]Department of Life Science, Mie University Graduate School of Bioresources, 1577 Kurimamachiya, Tsu, Mie 514-8507, Japan, [3]Glycobiology Research Group, Tokyo Metropolitan Institiute of Gerontology, Foundation for Research on Aging and Promotion of Human Welfare, 35-2 Sakaecho, Itabashi, Tokyo 173-0015, Japan, and [4]Laboratory of Applied Biotechnology, Mie University Venture Business Laboratory, 1577 Kurimamachiya,Tsu, Mie 514-8507, Japan

Received on November 26, 2008; revised on April 28, 2010; accepted on May 2, 2010

Two distinct cDNAs corresponding to two zebrafish protein *O*-mannosyltransferase genes, *zPOMT1* and *zPOMT2*, were cloned from early developmental embryos. Gene expression analysis revealed that *zPOMT1* and *zPOMT2* were expressed in similar patterns during early embryonic development and in all adult tissues. To study the regulation of *zPOMT1* and *zPOMT2* mRNA distribution during zebrafish embryogenesis, we injected *enhanced green fluorescent protein* (*EGFP*) mRNA fused to the 3′untranslated regions of each *zPOMT* gene. The distribution of EGFP resulting from the two constructs was similar. Injection of antisense morpholino oligonucleotides of *zPOMT1* and *zPOMT2* resulted in several severe phenotypes—including bended body, edematous pericaridium and abnormal eye pigmentation. Immunohistochemistry using anti-glycosylated α-dystroglycan antibody (IIH6) and morphological analysis revealed that the phenotypes of *zPOMT2* knockdown were more severe than those of *zPOMT1* knockdown, even though the IIH6 reactivity was lost in both *zPOMT1* and *zPOMT2* morphants. Finally, only when both *zPOMT1* and *zPOMT2* were expressed in human embryonic kidney 293T cells were high levels of protein *O*-mannosyltransferase activity detected, indicating that both zPOMT1 and zPOMT2 were required for full enzymatic activity. Moreover, either heterologous combination, *zPOMT1* and *human POMT2* (*hPOMT2*) or *hPOMT1* and *zPOMT2*, resulted in enzymatic activity in cultured cells. These results indicate that the protein *O*-mannosyltransferase machinery in zebrafish and humans is conserved and suggest that zebrafish may be useful for functional studies of protein *O*-mannosylation.

Keywords: development/glycosylation/POMT1 and POMT2/protein *O*-mannosyltransferase activity/zebrafish

Introduction

Posttranslational modification of proteins by glycosylation has critical biological functions at both the cellular and organismal levels (Haltiwanger and Lowe 2004; Ohtsubo and Marth 2006). In addition to the generally observed types of glycosylation such as *N*-glycosylation and mucin-type *O*-glycosylation, several unique glycans have recently been found to play important roles in a variety of biological processes. According to current knowledge, protein *O*-mannosylation in mammals is found on a relatively small number of proteins in the brain, nerves and skeletal muscle (Krusius et al. 1986; Chiba et al. 1997; Sasaki et al. 1998; Endo 1999). In contrast to yeast cells, where *O*-mannose is elongated by neutral, linear oligomannose chains (Strahl-Bolsinger and Tanner 1991), the mannose residue of mammalian *O*-mannosylglycans is extended with complex glycans terminating with sialic acid, sulfate or fucose (Endo 1999). The structure Siaα2-3Galβ1-4GlcNAcβ1-2Manα1-Ser/Thr is required for binding between α-dystroglycan (α-DG) and laminin G domain (Chiba et al. 1997; Endo 1999; Montanaro and Carbonetto 2003).

Muscular dystrophies are genetic diseases characterized by progressive muscle degeneration and muscular weakening. They can be classified into a number of disease types, and some causative genes have been identified (Burton and Davies 2002). For example, dystrophin forms a dystrophin–glycoprotein complex (DGC), and Duchenne muscular dystrophy is caused by mutations in the gene encoding dystrophin. Mutations in other components of DGC are involved in other muscular dystrophies. Defects in glycosylation of α-DG, one of the DGC components, are responsible for certain congenital muscular dystrophies (Endo and Toda 2003; Michele and Campbell 2003). These kinds of muscular dystrophies, including diseases such as Walker–Warburg syndrome (WWS) and muscle–eye–brain disease, are called α-dystroglycanopathies. Protein *O*-mannosyltransferases (POMT1 and POMT2) catalyze the first step in *O*-mannosyl glycan synthesis (Manya et al. 2004), and defects in human POMT1 (hPOMT1) or hPOMT2 result in WWS, an autosomal recessive disorder associated with severe congenital muscular dystrophy, abnormal

[1]To whom correspondence should be addressed: Tel:/Fax: +81-59-231-9560; e-mail address: ytamaru@bio.mie-u.ac.jp
[5]Present address: Department of Nephrology, Nagoya University Graduate School of Medicine, 65 Tsurumai, Showa, Nakagawa, Nagoya, Aichi 466-8550, Japan
*These authors contributed equally.

A

```
1    GAACAGACCGTTGCTTTATTTACAGTGTTTAGTGGCTTTATTTAAAGCGTAAAGTTGTCGTATATGCCTAAGCAATGGCATTATTTATTT   90
                                                                    M  Q  C  V  K  L  P  V  S  V
91   GTTTTTATTTTTCTTGACCAATTCCAGTTTTAGCGAATATTTTTATTCATAATTTACTGCTAAAAGACCGCGCATGTGGTCGTGAAAGCA  180
181  GCACTGTTCACCTATGATTGCGAAATTCCAGAGGAAAAACTGAATCAAGTCAGGATTGAGCATGCAGTGTGTTAAACTGCCCGTCAGTGT  270
     T  V  E  I  N  V  L  L  L  A  V  T  A  L  A  L  F  T  R  L  Y  G  I  H  F  P  K  A  V  V
271  GACAGTGGAGATAAATGTGCTGCTGCTGGCGGTTACAGCACTTGCCCTCTTTACTCGACTTTATGGCATTCACTTTCCCAAAGCTGTAGT  360
     T  V  E  I  N  V  L  L  L  A  V  T  A  L  A  L  F  T  R  L  Y  G  I  H  F  P  K  A  V  V
361  GTTTGATGAGGTTTATTATGGACAGTTCCTGTCATTGTACATGAAGCAGGTTTTTTTCATAGATGAAAGCGGTCCTCCTTTTGGACACAT  450
     F  D  E  V  Y  Y  G  Q  F  L  S  L  Y  M  K  Q  V  F  F  I  D  E  S  G  P  P  F  G  H  M
451  GATACTTGCTTTAGGAGCGTATTTAGGAGGATTTGATGGCAACTTTGTTTGGAACAGAATTGGAGCAGAATACCCTGGTAATGTCCCTGT  540
     I  L  A  L  G  A  Y  L  G  G  F  D  G  N  F  V  W  N  R  I  G  A  E  Y  P  G  N  V  P  V
541  TTGGAGCCTTCGACTGATACCGGCTCTAGCAGGCTCTTTTTGTGTGCCACTTGCATATCTTGTAGTAGTGGAGCTGGGATACTCCCACTT  630
     W  S  L  R  L  I  P  A  L  A  G  S  F  C  V  P  L  A  Y  L  V  V  V  E  L  G  Y  S  H  F
631  CTCGGCACTGGGGGCCTGTGCACTTCTCCTCATGGAAAACTCCCTGATTGTGCAATCGCGCTTCATGCTGCTGGAGTCTGTTTTAATTTT  720
     S  A  L  G  A  C  A  L  L  L  M  E  N  S  L  I  V  Q  S  R  F  M  L  L  E  S  V  L  I  F
721  CTTCTTGCTGTTGGCTGTGCTGTCTTACCTCCGCTTTCCCCAAGCACGCAACTCATTTTTCAAGTGGTTCTGGCTTGTGATCTGTGGGGT  810
     F  L  L  L  A  V  L  S  Y  L  R  F  P  Q  A  R  N  S  F  F  K  W  F  W  L  V  I  C  G  V
811  CAGCTGTGCATTCGGAATTGGGGTAAAGTACATGGGTATGTTCACATACTTTCTACTGCTGAGCCTGGCAGCTGTACACACCTGGCAGCT  900
     S  C  A  F  G  I  G  V  K  Y  M  G  M  F  T  Y  F  L  L  L  S  L  A  A  V  H  T  W  Q  L
901  TATTGGAGATCGAACCTTGAGCCATGGCAAAGTAATGTTCCAGGTATTAGTTCGCTTCTTGGCACTCGTGGTGCTACCTGTCATCATTTA  990
     I  G  D  R  T  L  S  H  G  K  V  M  F  Q  V  L  V  R  F  L  A  L  V  V  L  P  V  I  I  Y
991  CCTTGGGTTTTTCTACATTCACCTGACCTTGCTATATCGCAGTGGACCTTCTGACCAGATGATGAGCAGTGCCTTTCAAGCAAGTCTAGA 1080
     L  G  F  F  Y  I  H  L  T  L  L  Y  R  S  G  P  S  D  Q  M  M  S  S  A  F  Q  A  S  L  E
1081 GGGTGGTCTTGCCCGGATCACTCAGGGGCAGCCTTTAGATGTAGCGTTCGGCTCACAGGTCACTCTCCGCACAGTCTCCGGTAAACCTGT 1170
     G  G  L  A  R  I  T  Q  G  Q  P  L  D  V  A  F  G  S  Q  V  T  L  R  T  V  S  G  K  P  V
1171 GCCTTGTTGGCTTCACTCACACAAGGCCAACTATCCCATCAGGTATGAAAATGGCCGTGGAAGCTCCCACCAGCAGCAGGTGACCTGCTA 1260
     P  C  W  L  H  S  H  K  A  N  Y  P  I  R  Y  E  N  G  R  G  S  S  H  Q  Q  Q  V  T  C  Y
1261 TCCTTTCAAAGATGTCAACAACTGGTGGATTATCAAAGACCCTGGGCGGCAAAGTCTTGTGGTCAGCAGCCCACCCAGACCTGTCAGACA 1350
     P  F  K  D  V  N  N  W  W  I  I  K  D  P  G  R  Q  S  L  V  V  S  S  P  P  R  P  V  R  H
1351 TGGGGATATTATTCAGTTGCTGCATGGAATGACAACTCGCTACCTGAACACACATGATGTTGCAGCCCCCATGAGTCCTCACTCACAGGA 1440
     G  D  I  I  Q  L  L  H  G  M  T  T  R  Y  L  N  T  H  D  V  A  A  P  M  S  P  H  S  Q  E
1441 AGTTTCGGGCTATATTGACTTTAACGTGTCTATGCCAGCCCAGAATCTCTGGAGAGTGGATATTGTGAACAGGGAGTCTGAGAAAGAGAT 1530
     V  S  G  Y  I  D  F  (N)  V  S  M  P  A  Q  N  L  W  R  V  D  I  V  N  R  E  S  E  K  E  I
1531 CTGGAAGACCATTTTATCAGAGGTGCGACTAGTCCACGTGAACCACCTCAGCTGTTTTAAAGCTCAGTGGAGCCTCTCTGCCGGAGTGGGG 1620
     W  K  T  I  L  S  E  V  R  L  V  H  V  (N)  T  S  A  V  L  K  L  S  G  A  S  L  P  E  W  G
1621 TTTTAAACAGCTGGAGGTGGTGGGTGATAAGATTTATAAAGGCTACCAGCAGACCGGCATGTGGAACGTGGAGGAGCACCGCTATGGCAG 1710
     F  K  Q  L  E  V  V  G  D  K  I  Y  K  G  Y  Q  Q  T  G  M  W  N  V  E  E  H  R  Y  G  R
1711 AAGTCAGGAACCAAAGGAAAGGGAGTTGGAGCTGAAGTCTCCTACTCACAGCGATGTCAACAAAAATCTCACATTTATGGCCAAATTTCT 1800
     S  Q  E  P  K  E  R  E  L  E  L  K  S  P  T  H  S  D  V  N  K  (N)  L  T  F  M  A  K  F  L
1801 GGAGCTGCAGTGGAAGATGCTGACAGTAAAGAACGAAGAGTCAGAGCACAAATATAGTTCATCACCTCTTGAATGGATCACAATGGACAC 1890
     E  L  Q  W  K  M  L  T  V  K  N  E  E  S  E  H  K  Y  S  S  S  P  L  E  W  I  T  M  D  T
1891 CAACATTGCATATTGGCTTCATCCTTCAAGTAATGCACAGATTCACTTTATAGGCAATATTGTTACTTGGACCACTGGAAACATTACACT 1980
     N  I  A  Y  W  L  H  P  S  S  N  A  Q  I  H  F  I  G  N  I  V  T  W  T  T  G  (N)  I  T  L
1981 GGTTGTGTACTGTCTTCTGTTTTTAACATACTTACTAAGACGGAGGAGGAAAGTTGAAGACATTCCACAAGACTCTTGGGAACAGTTGGC 2070
     V  V  Y  C  L  L  F  L  T  Y  L  L  R  R  R  R  K  V  E  D  I  P  Q  D  S  W  E  Q  L  A
2071 TTTGGCTGGTGTGGTTTGCTTTGGAGGCTGGGCAGTGAATTACCTGCCATTCTTCCTAATGGAGAAGACTCTCTTTCTATATCACTATCT 2160
     L  A  G  V  V  C  F  G  G  W  A  V  N  Y  L  P  F  F  L  M  E  K  T  L  F  L  Y  H  Y  L
2161 CCCAGCACTCACCTTCAAGATCTTGCAAATACCTATAGTCACAGAGCACCTGTACATCCACGTATTGAGATCCTCAGCTCAACAGAAAGC 2250
     P  A  L  T  F  K  I  L  Q  I  P  I  V  T  E  H  L  Y  I  H  V  L  R  S  S  A  Q  Q  K  A
2251 ATTTGGTGGTGTGATTTTAGCAGTTCTTTGTTCAGTATACATGTCCTACCACAGCTTGAGTCCTCTCACGTATGGCCAGCCAGCGTTAAC 2340
     F  G  G  V  I  L  A  V  L  C  S  V  Y  M  S  Y  H  S  L  S  P  L  T  Y  G  Q  P  A  L  T
2341 ATCAGACAAGCTCGCTGAGCTGCGCTGGAGGGAGAGTTGGGATATTCTCTTACGCAAACGCTAAAATATCCTTTATTTTTTTTAAGACAA 2430
     S  D  K  L  A  E  L  R  W  R  E  S  W  D  I  L  L  R  K  R  *
2431 GATAATTTCATGGTGTCAAAATTTTAAATCGAGATGACTGATAGGGCTGATGGATTTTTTGAGAAATGGATTCTGATTCGAAATGCATCA 2520
2521 CTTTTCTGTCTTGAATGGATTCTGAGCTCAGTGTTTAACAGGAGATTATACCATATGCTTTACAAACTCTGCTTGCTTCCAATTCCTTAC 2610
2611 AAATACCACATGAATCTAAAGTAATCAGTAATGAAGTTCAAATTAGCCAATTACAAAAGTGTTTTTAGTGAGCTGTTTACATTAATCTTG 2700
2701 TCATAAAGGCCAACTTACATGAAGCACAAGCAATATATGGTTTGAAAACTAGTCAAGAGTGCAACATGCTGTTAAAAACTAAGTTTAGAA 2790
2791 TCACTTCAAGAGAGAATAGCAACGCATTTTGAATCAATTTTTCAATATTACACCATAGTTTTCATGGATTTCCAGAAAGCTGTGAAGCAC 2880
2881 TATTTCTAGGGTCTGTGCCCAAACATAATAATGTGAAAAAAAACTCATGCTGCTGAATCTGAAAACTCTAAACCAAATGGACTCTGAAGC 2970
2971 ACAATTTCCGTGCTACATTTATCATGCTCGTATGTTTACATATTACTCTGTTTGTATAGCGATTTTATTGTATTGTTTTAGAGACTGTTA 3060
3061 AACTAATAAGATGCATTGCATTTCTTTAAATATGTTTTATTTGATTCTTGCACAACAGAAAAAAACGTTTAATAAACGTTTATATGACAT 3150
3151 TAAAAAAAAAAAAAAAAAA                                                                        3169
```

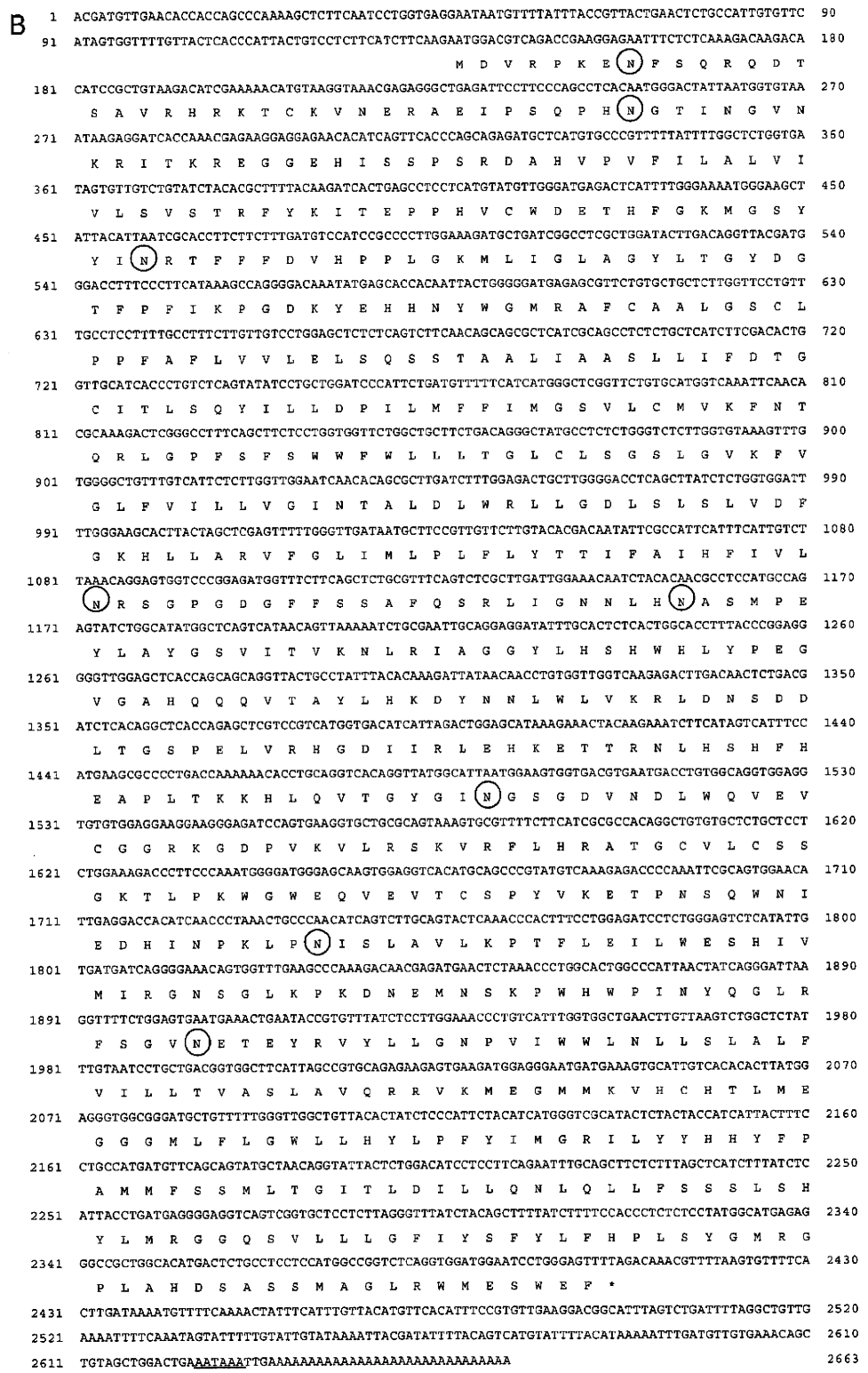

Fig. 1. Nucleotide sequences and deduced amino acid sequences of *zPOMT1* and *zPOMT2*. The cDNA sequences of zebrafish *POMT1* (**A**) and *POMT2* (**B**) genes are presented on the upper line. Deduced amino acid sequences are indicated by the single-letter amino acid codes. Potential *N*-glycosylation sites are indicated by circles. Consensus polyadenylation sites are underlined.

neuronal migration and eye anomalies (Beltran-Valero de Bernabe et al. 2002; van Reeuwijk et al. 2005). POMT orthologs have been identified in many animals, including *Drosophila* (Martín-Blanco and García-Bellido 1996; Willer et al. 2002), mouse (Willer et al. 2002; Willer et al. 2004), rat (Manya et al. 2006) and humans (Jurado et al. 1999; Willer et al. 2002). *Drosophila*, rat and mouse have orthologs of both of human *POMT* genes, and their products have protein *O*-mannosyltransferase activity when only they are co-expressed (Ichimiya et al. 2004; Manya et al. 2006; Lommel et al. 2008). In contrast, *Drosophila* does not have orthologs to human or murine protein *O*-mannose β1,2-*N*-acetylglucosaminyltransferase1 (POMGnT1) (Ichimiya et al. 2004). POMGnT1 catalyzes the transfer of GlcNAc from UDP-GlcNAc to the protein *O*-mannosyl residue (Yoshida et al. 2001; Liu et al. 2006; Miyagoe-Suzuki et al. 2009). Therefore, it seems that the structures of *O*-mannosylglycans of invertebrates are quite different from those of vertebrates. Moreover, it has been reported that hPOMT1 and hPOMT2 must form a heterocomplex for protein *O*-mannosyltransferase activity (Akasaka-Manya et al. 2006).

The zebrafish (*Danio rerio*) provides a readily accessible model for human muscle diseases such as muscular dystrophies (Bassett and Currie 2003). Muscle specification and differentiation follow a well-characterized time course and allow detailed analysis with single-cell resolution (Devoto et al. 1996). Zebrafish orthologs of proteins in the human DGC have been implicated in muscle development, and some zebrafish DGC orthologs have uses as models to study human muscular dystrophy and congenital myopathy (Parsons et al. 2002; Bassett and Currie 2003; Guyon et al. 2003). More recently, it has been reported that the zebrafish has orthologs of *POMT1*, *POMT2*, *POMGnT1* and other putative glycosyltransferases expected to contribute to the synthesis of mammalian-type *O*-mannosylglycan (Steffen et al. 2007; Moore et al. 2008). Taken together, the structures of *O*-mannosylglycans are thought to be similar in diverse vertebrates. Therefore, zebrafish may be a useful model for analyses of the biosynthetic

A

```
hPOMT1   1:----------------------MWGFLKRPVVVTADINLSLVALTGMGLLSRLWRLTYPRAVVFDEVYYGQYISFYMKQIFFLDDSGPPF  68
mPOMT1   1:MGSHSTGLEETLGVLPSWLFCKMLRFLKRPLVVTVDINLNLVALTGLGLLTRLWQLSYPRAVVFDEVYYGQYISFYMKRIFFLDDSGPPF  90
rPOMT1   1:MGNRSMGREDTLGVLPSLLFCKMLRFLKRPLVVTIDINLNLVALTVLGLLTRLWQLSYPRAVVFDEVYYGQYISFYMKRVFFLDDSGPPF  90
zPOMT1   1:----------------------MQ-CVKLPVSVTVEINVLLLAVTALALFTRLYGIHFPKAVVFDEVYYGQFLSLYMKQVFFTDESGPPF  67

hPOMT1  69:GHMVLALGGYLGGFDGNFLWNRIGAEYSSNVPVWSLRLLPALAGALSVPMAYQIVLELHFSHCAAMGAALLMLIENALITQSRLMLLESV 158
mPOMT1  91:GHMLLALGGWLGGFDGNFLWNRIGAEYSSNVPIWSLRLLPALAGALSVPMAYQIVLELHFSHGAAIGAALLMLIENALITQSRLMLLESI 180
rPOMT1  91:GHMLLALGGWLGGFDGNFLWNRIGAEYSSNVPVWSLRLLPALAGALSVPMAYQIVLELHFSHCTAMGAALLMLIENALITQSRLMLLESI 180
zPOMT1  68:GHMILALGAYLGGFDGNFVWNRIGAEYPGNVPVWSLRLIPALAGSFCVPLAYLVVVELGYSHFSALGACALLLMENSLIVQSRFMLLESV 157

hPOMT1 159:LIFFNLLAVLSYLKFFNCQKHSPFSLSWWFWLTLTGVACSCAVGIKYMGVFTYVLVLGVAAVHAWHLLGDQTLSNVCVFCHLLARAVALL 248
mPOMT1 181:LIFFNLLAVLSYLKFFNSQTHSPFSVHWWLWLLLTGVSCSCAVGIKYMGIFTYLLVLGIAAVHAWNLIGDQTLSNMRVLSHLLARIVALL 270
rPOMT1 181:LIFFNLLAVLSYLKFFNSQTHSPFSVHWWLWLMLTGVSCSCAVGIKYMGIFTYLLVLSIAAVHAWHLIGDQTLSNICVLSHLLARAVALL 270
zPOMT1 158:LIFFLLLAVLSYLRFHKARN----SFFKWFWLVICGVSCAFGIGVKYMGMFTYFLLLSLAAVHTWQLIGDRTLSHGKVMFQVLVRFLALV 243

hPOMT1 249:VIPVVLYLLFFYVHLILVFRSGPHDQIMSSAFQASLEGGLARITQGQPLEVAFGSQVTLRNVFGKPVPCWLHSHQDTYPMIYENGRGSSH 338
mPOMT1 271:VVPVFLYLLFFYVHLMLLYRSGPHDQIMSSAFQASLEGGLARITQGQPLEVAFGSQVTLKSVSGKPLPCWLHSHKNTYPMIYENGRGSSH 360
rPOMT1 271:VVPVFLYLLFFYVHLMLLYRSGPHDQIMSSAFQASLEGGLARITQGQPLEVAFGSQVTLKSVSGKPLPCWLHSHKNTYPMIYENGRGSSH 360
zPOMT1 244:VLPVIIYLGFFYIHLTLLYRSGPSDQMMSSAFQASLEGGLARITQGQPLDVAFGSQVTLRTVSGKPVPCWLHSHKANYPIRYENGRGSSH 333

hPOMT1 339:QQQVTCYPFKDVNNWWIVKDPRRHQLVVSSPPRPVRHGDMVQLVHGMTTRSLNTHDVAAPLSPHSQEVSCYIDYNISMPAQNLWRLEIVN 428
mPOMT1 361:QQQVTCYPFKDINNWWIVKDPGRHQLVVNNPPRPVRHGDIVQLVHGMTTRLLNTHDVAAPLSPHSQEVSCYIDYNISMPAQNLWKLDIVN 450
rPOMT1 361:QQQVTCYPFKDINNWWIVKDPGRHQLVVNNPPRPVRHGDIVQLVHGMTTRLLNTHDVAAPLSPHSQEVSCYIDYNISMPAQNLWKLDIVN 450
zPOMT1 334:QQQVTCYPFKDVNNWWIIKDPGRQSLVVSSPPRPVRHGDIIQLLHGMTTRYLNTHDVAAPMSPHSQEVSGYIDFNVSMPAQNLWRVDIVN 423

hPOMT1 429:RGSDTDVWKTILSEVRFVHVNTSAVLKLSGAHLPDWGYRQLELVGEKLSRGYHGSTVWNVEEHRYGASQEQRERERELHSPAQVDVSRNL 518
mPOMT1 451:RESNRDTWKTILSEVRFVHVNTSAILKLSGAHLPDWGFRQLEVVGEKLSPGYHESMVWNVEEHRYGKSHEQKERELELHSPTQLDISRNL 540
rPOMT1 451:RESNQDTWKTILSEVRFVHVNTSAILKLSGAHLPDWGFRQLEVVGEKLSLGPHESMVWNVEEHRYGRGHEQKERELELHSPTQHDISRNL 540
zPOMT1 424:RESEKEIWKTILSEVRLVHVNTSAVLKLSGASLPEWGFKQLEVVGDKIYKGYQQTGMWNVEEHRYGRSQEPKERELELKSPTHSDVNKNL 513

hPOMT1 519:SFMARFSELQWRMLALRSDDSEHKYSSSPLEWVTLDTNIAYWLHPRTSAQIHLLGNIVIWVSGSLALAIVALLSLWYLLRRRRNVHDLPQ 608
mPOMT1 541:SFMARFSELQWKMLTLKNEDLEHQYSSTPLEWLTLDTNIAYWLHPRTSAQIHLLGNIVIWTSASLATVVYTLLFFWYLLRRRRSICDLPE 630
rPOMT1 541:SFMARFSELQWKMLTLKNEDLEHQYSSTPLEWLTLDTNIAYWLHPRTSAQIHLLGNIVIWTSASLATVAYTLLFFWYLLRRRRNICDLPE 630
zPOMT1 514:TFMAKFLELQWKMLTVKNEESEHKYSSSPLEWITMDTNIAYWLHPSSNAQIHFIGNIVTWTTGNITLVVYCLLFLTYLLRRRRKVEDIPQ 603

hPOMT1 609:DAWLRWVLAGALCAGGWAVNYLPFFLMEKTLFLYHYLPALTFQILLLPVVLQHISDHLCRSQLQRSIFSALVVAWYSSACHVSNTLRPLT 698
mPOMT1 631:DAWSRWVLAGALCTGGWALNYLPFFLMERVLFLYHYLPALTFQILLLPIVLQHASDHLCRSQLQRNVFSALVVAWYSSACHVSNMLRPLT 720
rPOMT1 631:DAWSHWVLAGALCIGGWALNYLPFFLMERMLFLYHYLPALTFQILLLPIVMQHASDHLCRSQLQRNVFSALVVAWYSSACHVSNMLRPLT 720
zPOMT1 604:DSWEQLALAGVVCFGGWAVNYLPFFLMEKTLFLYHYLPALTFKILQIPIVTEHLYIHVLRSSAQQKAFGGVILAVLCSVYMSYHSLSPLT 693

hPOMT1 699:YGDKSLSPHELKALRWKDSWDILIRKH                                                              725
mPOMT1 721:YGDTSLSPGELRALRWKDSWDILIRK                                                               746
rPOMT1 721:YGDTSLSPGELRALRWKDSWDILIRKY                                                              747
zPOMT1 694:YGQPALTSDKLAELRWRESWDILLRKR                                                              720
```

B

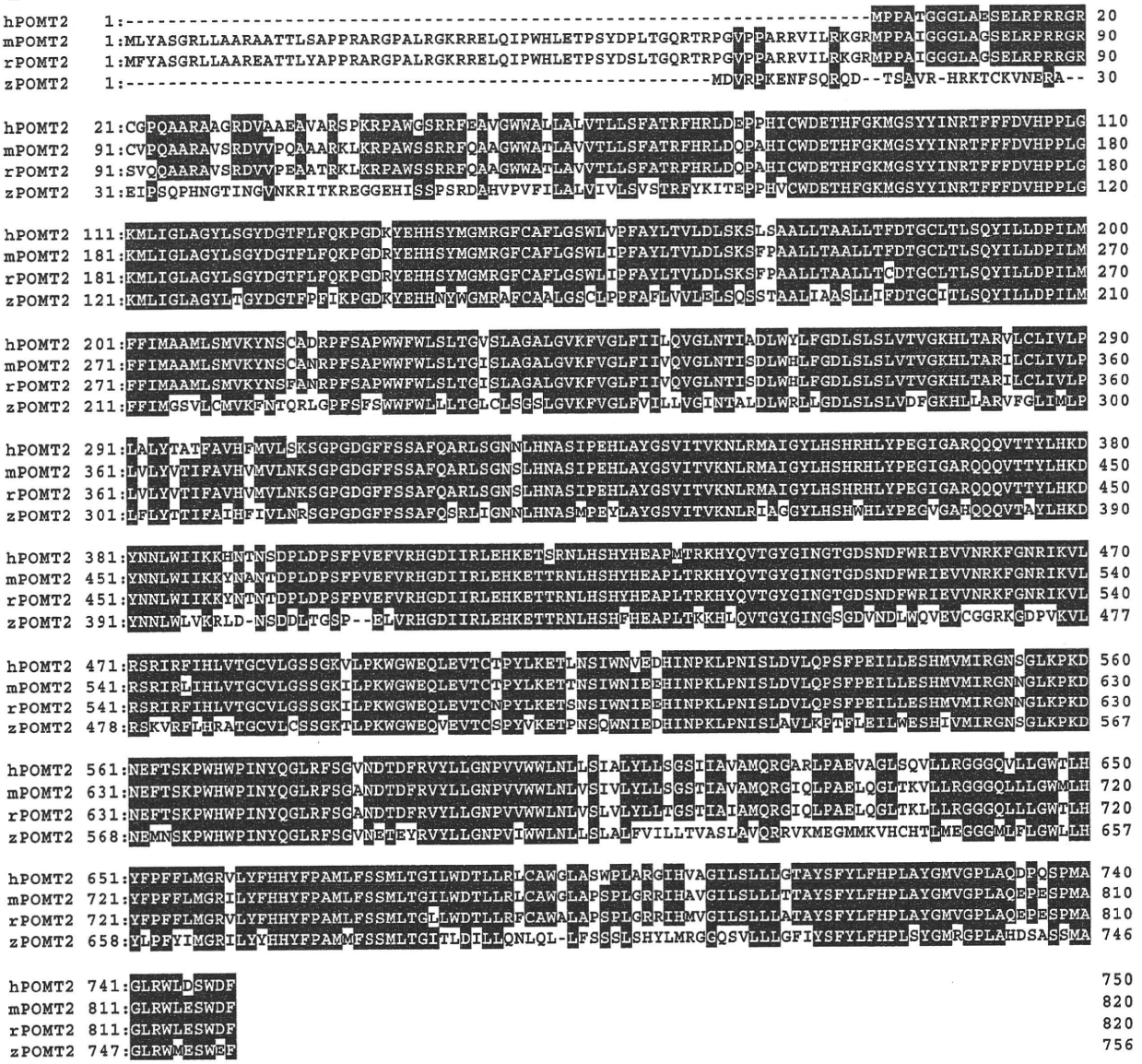

pathway of *O*-mannosylglycans in vertebrates, the mechanisms of muscular dystrophies, and myogenesis.

In this study, we isolated and cloned full-length cDNAs encoding two zebrafish *POMT* genes, *zPOMT1* and *zPOMT2*, and examined whether they have protein *O*-mannosyltransferase activity. We also investigated the expression patterns of both genes during embryogenesis and in adult tissues. Furthermore, we analyzed the distribution and localization of a protein expressed from constructs containing the 3′untranslated region (3′UTR) of *zPOMT1* or *zPOMT2*. Finally, knockdown analysis using antisense morpholino oligonucleotides (MOs) was performed to assess the function of protein *O*-mannosylation during zebrafish development.

Results

cDNA cloning and sequencing of zPOMT1 and zPOMT2

The full-length cDNAs encoding *zPOMT1* and *zPOMT2* genes were cloned by reverse transcriptase-polymerase chain reaction (RT-PCR) using zebrafish embryos. The complete cDNAs and deduced amino acid sequences of *zPOMT1* and *zPOMT2* are shown in Figure 1 (GenBank accession nos. AB281275 and AB281276, respectively). *zPOMT1* consisted of an open reading frame (ORF) of 2160 bases encoding a conceptual translation product of 720 amino acids with a predicted molecular mass of 82,036 Da (Figure 1A). *zPOMT2* consisted of an ORF of 2268 bases encoding conceptual translation product of 756 residues with a predicted molecular mass of 85,710 Da

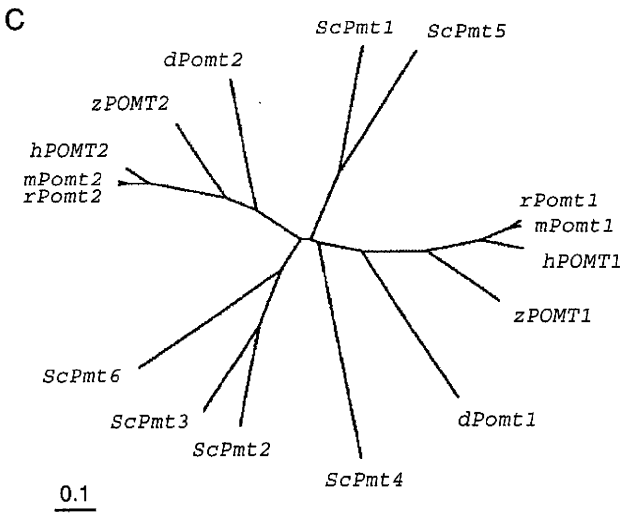

Fig. 2. Comparisons of human, mouse, rat and zebrafish POMTs. ClustalW alignments of human (h), mouse (m), rat (r) and zebrafish (z) POMT1 (**A**) and POMT2 (**B**) amino acid sequences are indicated by single-letter amino acid codes, respectively. Conserved amino acids are highlighted. (**C**) ClustalW phylogenic tree of human, mouse, rat, zebrafish and *Drosophila* (d) POMTs and *S. cerevisiae* (Sc) Pmts. The amino acid sequence of hPOMT1 is a major type that was used for assay of protein *O*-mannosyltransferase activity in this study. The amino acid sequences of mPOMT2 and rPOMT2 belonged to the testis form. The branch lengths indicate amino acid substitutions per site.

(Figure 1B). A consensus polyadenylation site (AATAAA) was located downstream of the translation termination codon in both *zPOMT1* and *zPOMT2*. As shown in Figure 2, the deduced amino acid sequences in both zPOMT1 and zPOMT2 were similar to those of mammals such as human, mouse and rat (Jurado et al. 1999; Willer et al. 2002; Willer et al. 2004; Manya et al. 2006). zPOMT1 had 66% identity to hPOMT1 (Figure 2A), whereas zPOMT2 showed 70% identity to hPOMT2 (Figure 2B). A phylogenetic analysis of 16 proteins—six *Saccharomyces cerevisiae* Pmts (ScPmt1-6) (Willer et al. 2002), two human (hPOMT1 and hPOMT2), two mouse (mPOMT1 and mPOMT2), two rat (rPOMT1 and rPOMT2), two *Drosophila* (dPOMT1 and dPOMT2) and two zebrafish (zPOMT1 and zPOMT2)—indicates that zPOMT1 is in the pmt4 subfamily and zPOMT2 is in the pmt2 subfamily (Figure 2C).

Gene expression of zPOMT1 and zPOMT2

Quantitative PCR was performed with early developmental stages (Figure 3A) and all adult tissues (Figure 3B). There were significant differences in the levels of *zPOMT1* and *zPOMT2* expression during embryogenesis. At 0 h post fertilization (hpf), both genes, *zPOMT1* and *zPOMT2*, were highly expressed. While *zPOMT1* expression decreased after 6 hpf, *zPOMT2* expression increased at 6 hpf and then decreased at 12 hpf. Furthermore, *zPOMT2* expression increased again around 24 hpf. There were no significant differences in *zPOMT1* and *zPOMT2* expression levels in males and females in any adult tissue except for the liver. Interestingly, *zPOMT1* and *zPOMT2* were highly expressed in both testis and ovary (Figure 3B). By means of whole-mount in situ hybridization, mRNAs of *zPOMT1* and *zPOMT2* were detected during early developmental stages. Both *zPOMT1* (Figure 3C) and *zPOMT2* (Figure 3D) transcripts were ubiquitously expressed throughout the gastrulation, tailbud and somite stages. At 24 hpf, both *zPOMT1* and *zPOMT2* mRNAs were detected predominantly in eyes and somites.

Localization of 3′UTRs in zPOMT1 and zPOMT2

The 3′UTR of an mRNA can affect the expression and/or localization of the mRNA during development within particular cells, including primary germ cells (Hashimoto et al. 2009). Therefore, to investigate the function of 3′ UTRs of *zPOMT1* and *zPOMT2*, we fused the 3′UTR of each *zPOMT* to the *enhanced green fluorescent protein* (*EGFP*) gene (Figure 3E). Capped mRNAs of *EGFP*-3′UTR of *zPOMT1* and *zPOMT2* were synthesized and injected into embryos at the one- to two-cell stage. With both constructs, EGFP was distributed throughout the whole body at 6 hpf, and EGFP was highly expressed in the eye, hindbrain and somite from 18 to 24 hpf (Figure 3F).

Knockdown analysis of zPOMT1 and zPOMT2

Antisense MOs against *zPOMT1* and *zPOMT2* were injected into the zebrafish embryos at the one- to two-cell stage, and the developmental progress of the morphants was compared with that of uninjected and control MO embryos (Figure 4). There were no significant differences between control MO and morphant embryos until 12 hpf. At 18 hpf, both *zPOMT1* MO and *zPOMT2* MO embryos were developmentally delayed in comparison with control MO (Figure 4A) and uninjected (data not shown) embryos. At 48 and 72 hpf, *zPOMT1* morphants showed slightly curved tails and curvature of the somite boundaries. In contrast, *zPOMT2* morphants at the same stage showed more severe phenotypes—including twisted tails, aberrant pericardium and abnormal eye pigmentation—than did the *zPOMT1* morphants. Quantitative analyses of embryos from all treatment groups were performed at 96 hpf. Each

Fig. 3. Gene expressions and whole-mount in situ hybridization for *zPOMT1* and *zPOMT2*. Quantitative PCR analyses of *zPOMT1* and *zPOMT2* mRNAs during early developmental stages (**A**) and in adult tissues (**B**). PCR products of *zPOMT1* and *zPOMT2* were detected throughout early developmental stages and in all tissues predominantly in gonads. *zβ-actin2* and *zCox1* were used as internal controls for quantitative PCR in early developmental stages and adult tissues, respectively. B, brain; E, eye; H, heart ; M, muscle ; T, testis; O, ovary; LM, liver (male); LF, liver (female); IM, intestine (male); IF, intestine (female); KM, kidney (male); KF, kidney (female); SM, spleen (male); SF, spleen (female). All reactions were performed in triplicate, and average values ± SD are shown. *zPOMT1* (**C**) and *zPOMT2* (**D**) mRNAs were detected. Both genes were expressed ubiquitously throughout early developmental stage, and high levels of expression were detected at 24 hpf. Arrowheads and boxes shown in the right columns at 24 hpf indicate eyes and the central parts of the somites, respectively. Boxes in 24 hpf were enlarged and shown in the far right panels. Scale bars = 100 μm. Illustration of capped mRNA structure (**E**) and localization of *EGFP*-3′UTR of control (upper panel), *zPOMT1* (middle panel) and *zPOMT2* (lower panel) (**F**). Arrows and arrowheads indicate the proteins corresponding to EGFP-*zPOMTs* 3′UTR. At 24 hpf, EGFP-3′UTR of *zPOMT1* was located predominately to the eye (arrowhead), whereas EGFP-3′UTR of *zPOMT2* was expressed highly in eye (arrowhead), hindbrain (arrow), and somite (bracket). Scale bars = 100 μm.

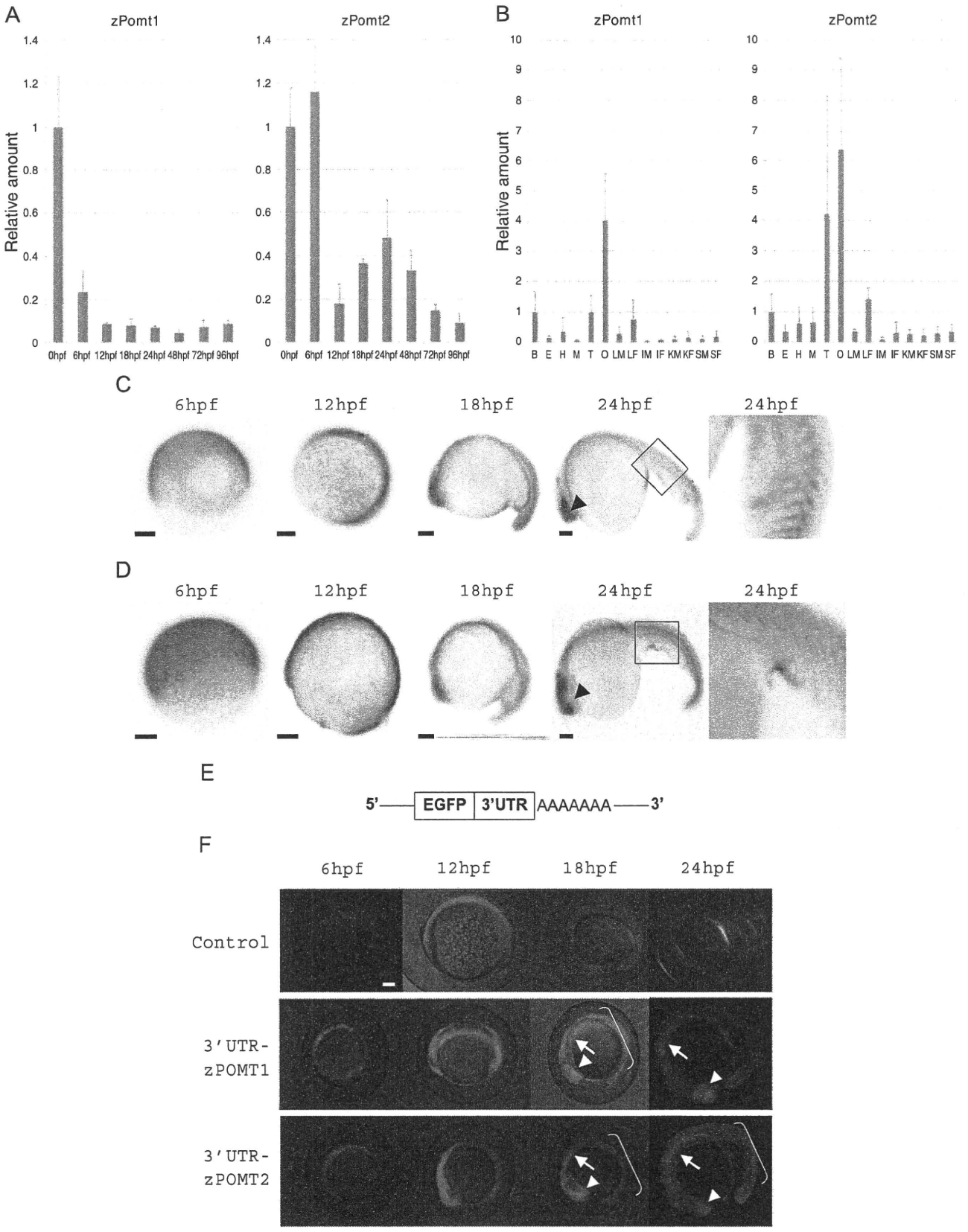

embryo with or without MO treatment was categorized as having normal, moderate or severe phenotypes according to morphological characteristics (Table I). The frequency of moderate and severe phenotypes increased with injection of increasing amounts of *zPOMT1* and *zPOMT2* MOs. The *zPOMT2* MO embryos had more severe deformities than did the *zPOMT1* MO embryos (Figure 4B, Table I). For example, aberrant eye pigmentation was observed only in *zPOMT2* MO embryos. Finally, swim bladders were not completely formed in *zPOMT1* and *zPOMT2* morphant embryos in comparison with uninjected or control MO embryos (Figure 4B).

To investigate the glycosylation status of α-DG in *zPOMT1* and *zPOMT2* morphant embryos, we immunostained embryos at 48 hpf with the anti-glycosylated α-DG antibody IIH6 (Figure 4C). Strong signals were detected with IIH6 in untreated embryos. Moreover, IIH6 reactivity in control MO embryos was also detected in the horizontal and vertical myosepta. However, the reactivity was almost completely lost in *zPOMT1* and *zPOMT2* morphants.

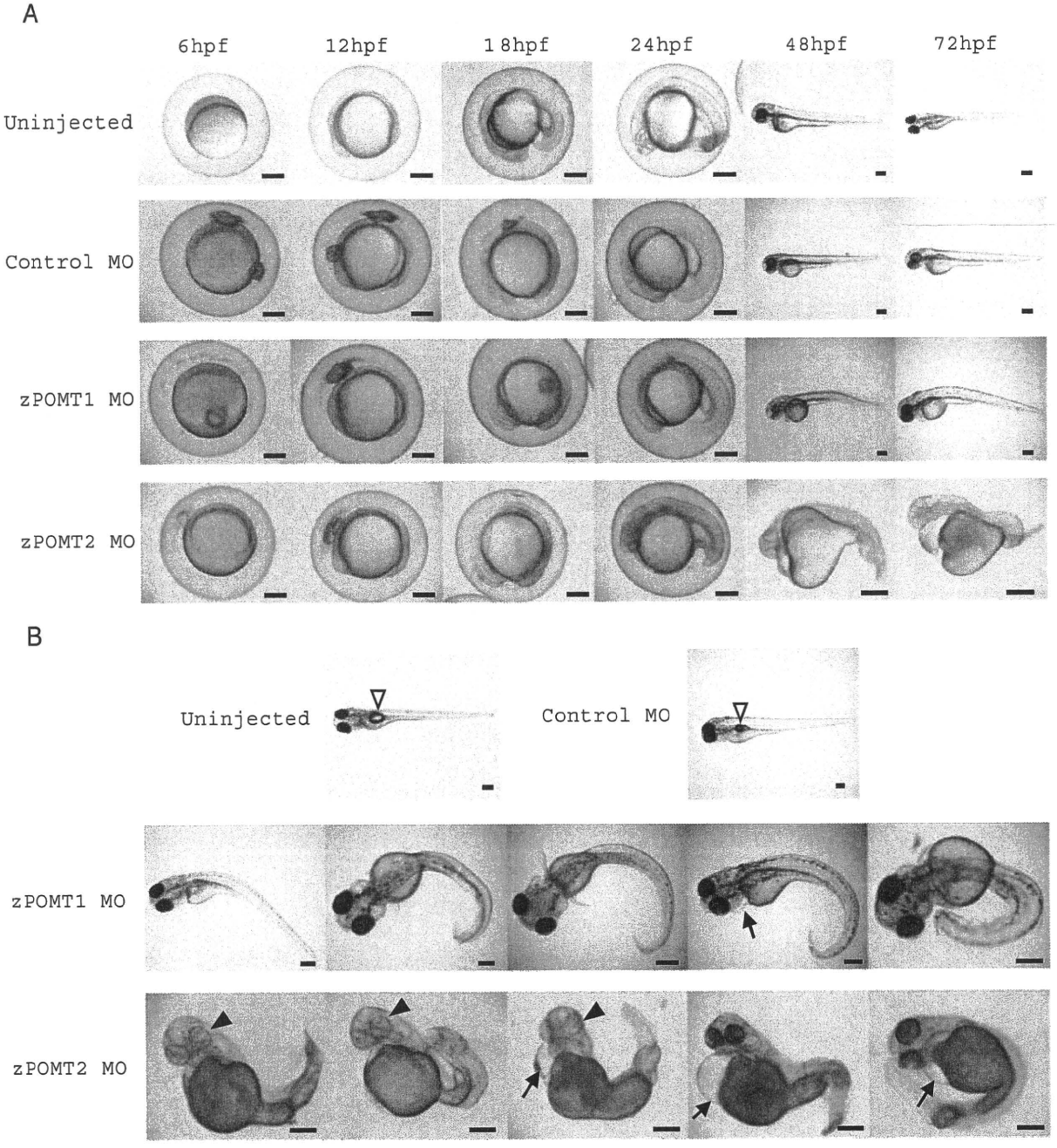

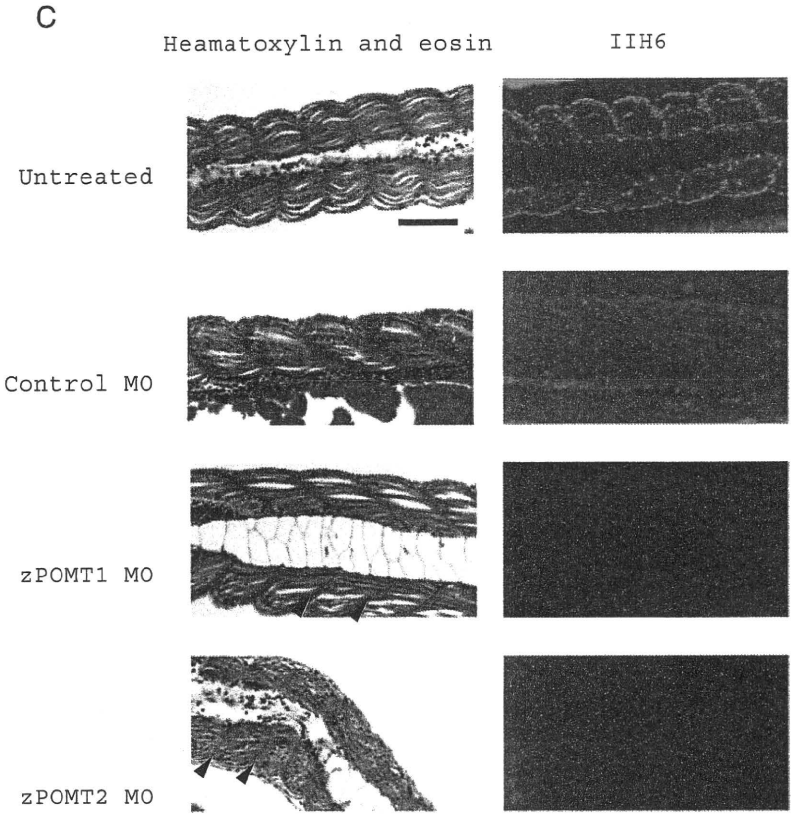

Fig. 4. Knockdown analysis of *zPOMT1* and *zPOMT2*. (**A**) Sequential changes during early developmental stages (6–72 hpf) of uninjected embryos (top panel), embryos injected with control MO (middle upper panel), embryos injected with *zPOMT1* MO (middle lower panel) and embryos injected with *zPOMT2* MO (bottom panel). Zebrafish embryos were injected with each MO at the one- to two-cell stage and were observed at 6, 12, 18, 24, 48 and 72 hpf. Scale bars = 200 μm. (**B**) 96 hpf morphants. Top panel: uninjected embryo (left side) and injected control MO (right side), embryos injected *zPOMT1* MO (middle panel), and embryos injected *zPOMT2* MO (bottom panel). Zebrafish embryos were injected with each MO at the one- to two-cell stages and were observed at 96 hpf. White arrowheads indicate swim bladder. Both morphant embryos revealed curved tail, and some had abnormal pericardium (arrows). Some of the *zPOMT2* morphants showed aberrant eye pigmentation (arrowheads). Scale bars = 200 μm. (**C**) Whole-mount immunohistochemistry with anti-glycosylated α-DG antibody IIH6 in 48-hpf embryos. Left panels, hematoxylin and eosin staining; right panels, IIH6 staining. IIH6 immunoreactivity was detected in uninjected and control MO but decreased in *zPOMT1* and *zPOMT2* morphants. Arrowheads represent vertical myosepta. Scale bars = 50 μm.

Protein O-mannosyltransferase activity of zPOMT1 and zPOMT2

To analyze the protein *O*-mannosyltransferase activity of zPOMT1 and zPOMT2, the cDNAs were cloned into an expression vector. The resulting expression constructs were transfected into human embryonic kidney 293T (HEK293T) cells, and microsomal membranes were used for enzyme assay. High levels of protein *O*-mannosyltransferase activity was observed only when the *zPOMT1* and *zPOMT2* genes were co-expressed in HEK293T cells (Figure 5). Jack bean α-mannosidase digestion showed that the mannosyl residue was linked to GST-α-DG by α-linkage (data not shown), as reported previously (Manya et al. 2004). Although a single transfection of *zPOMT1* in HEK293T cells did not show any enzymatic activity, transfection of *zPOMT2* alone did result in low levels of activity. Cells co-transfected with *zPOMT1* and *hPOMT2* and cells co-transfected with *hPOMT1* and *zPOMT2* showed robust levels of *O*-mannosyltransferase activity. In contrast, cells co-transfected with *zPOMT1* and *hPOMT1* and cells co-transfected with *zPOMT2* and *hPOMT2* did not show any enzymatic activity (data not shown). These results indicated that POMT1 and POMT2 from zebrafish and humans are interchangeable and that POMT1 and POMT2 have different functional roles in POMT enzymatic activity.

Table I. Quantification of *zPOMT* morphant phenotypes at 96 hpf

	Concentration (mM)	Normal	Moderate	Severe
Uninjected	-	97 (100.0%)	0 (0%)	0 (0%)
Control MO	1.0	65 (95.6%)	3 (4.4%)	0 (0%)
zPOMT1 MO	1.0	65 (79.3%)	14 (17.1%)	3 (3.6%)
	0.5	72 (93.5%)	4 (5.2%)	1 (1.3%)
	0.25	72 (98.6%)	0 (0%)	1 (1.4%)
zPOMT2 MO	1.0	33 (35.5%)	31 (33.3%)	29 (31.2%)
	0.5	55 (61.1%)	26 (28.9%)	9 (10.0%)
	0.25	79 (86.8%)	5 (5.5%)	7 (7.7%)

The phenotypic data shown were obtained from three independent experiments. The number of embryos observed for each phenotypic class is shown and also presented as a percentage of the total number of embryos studied for each morpholino (MO). Moderate (curved tails and curvature of the somite boundaries); Severe (twisted tail and aberrant pericardium).

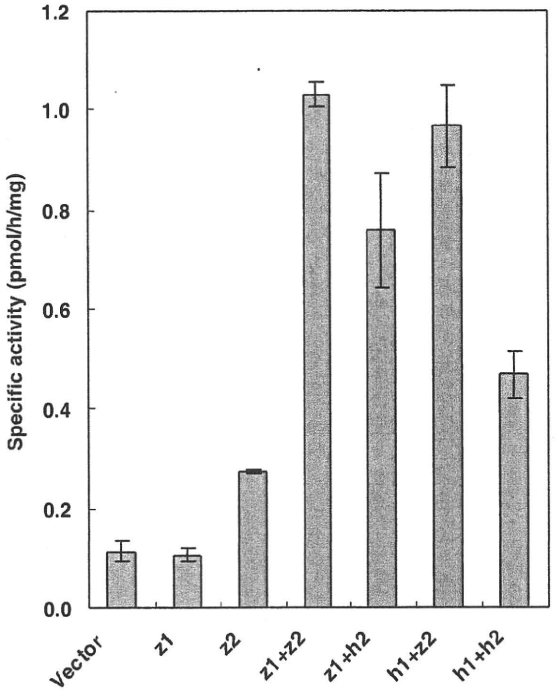

Fig. 5. Protein *O*-mannosyltransferase activities of *zPOMTs*. Protein *O*-mannosyltransferase activity was based on the rate of mannose transfer from mannosylphosphoryldolichol to a GST-α-DG. Vector, cells transfected with vector only; z1, cells transfected with *zPOMT1*; z2, cells transfected with *zPOMT2*; z1+z2, cells co-transfected with *zPOMT1* and *zPOMT2*; z1+h2, cells co-transfected with *zPOMT1* and *hPOMT2*; h1+z2, cells co-transfected with hPOMT1 and *zPOMT2*; h1+h2, cells co-transfected with *hPOMT1* and *hPOMT2*. Average values ± SD of three independent experiments are shown.

Discussion

Zebrafish have been useful for the study of human muscular dystrophies and congenital myopathies (Parsons et al. 2002; Bassett and Currie 2003; Bassett et al. 2003; Guyon et al. 2003) because zebrafish have orthologs of genes implicated in human muscular dystrophies, including *POMT1*, *POMT2*, *POMGnT1*, *dystrophin*, *fukutin* and fukutin-related protein (*FKRP*) (Steffen et al. 2007; Moore et al. 2008). Recently, it has been reported that knockdown analysis of *FKRP*, one of the causative genes in α-dystroglycanopathies, resulted in morphants that showed a pathological spectrum similar to those of human muscular dystrophies associated with mutations in *FKRP* (Thornhill et al. 2008). However, the function of FKRP is not clear yet (Esapa et al. 2002; Esapa et al. 2005; Matsumoto et al. 2004; Dolatshad et al. 2005; Torelli et al. 2005; Beedle et al. 2007). In contrast, POMTs are known to be protein *O*-mannosyltransferases. *FKRP* MO and *zPOMTs* morphant embryos showed a reduction in the glycosylated α-DG staining, indicating that FKRP may affect the biosynthetic pathway of *O*-mannosylglycans (Thornhill et al. 2008).

In mammals, two protein *O*-mannosyltransferase (POMTs) family members, POMT1 and POMT2, are known to exist. hPOMT1 and hPOMT2 catalyze protein *O*-mannosyl transfer to α-DG, which serves as a protein substrate, and mutations in the *hPOMT1* and *hPOMT2* genes result in WWS, a severe muscular dystrophy that also results in structural alterations in eyes and brain malformations, such as cobblestone lissencephaly. In this study, we have identified, cloned and expressed the full-length cDNAs of the *zPOMT1* and *zPOMT2* genes, and our results suggest that high levels of protein *O*-mannosyltransferase activity depends on expression of both genes. Co-expression of both *zPOMT1* and *zPOMT2* genes showed high protein *O*-mannosyltransferase activity similar to results from analyses of hPOMTs. Although transfection of *zPOMT1* alone did not show any enzymatic activity, transfection of *zPOMT2* alone showed slight activity. These results suggest that zPOMT2 itself has enzymatic activity, or zPOMT2 may form a complex with endogenous hPOMT1 resulting in low levels of enzymatic activity. Two heterologous protein combinations, zPOMT1 and hPOMT2 or zPOMT2 and hPOMT1, resulted in robust levels of enzymatic activity (Figure 5). This result suggests that a single mechanism of *O*-mannosylation is common to humans and zebrafish. On the other hand, cells co-transfected with *zPOMT1* and *hPOMT1* and cells co-transfected with *zPOMT2* and *hPOMT2* did not show any enzymatic activity, indicating clearly that POMT1 and POMT2 have different functional roles in POMT enzymatic activity. It is not clear why protein *O*-mannosyltransferase activity requires co-expression of POMT1 and POMT2 (Ichimiya et al. 2004; Manya et al. 2006; Manya et al. 2004); this study). One possibility is that POMT1 is a catalytic molecule and POMT2 is a regulatory molecule or vice versa. Another possibility is that assembly of POMT1 and POMT2 forms a catalytic domain. To further understand the mechanism of protein *O*-mannosylation, it is necessary to perform a structural study of a complex formed by POMT1 and POMT2.

Remarkably, overlapping expression patterns of *zPOMT1* and *zPOMT2* were observed by whole-mount in situ hybridization (Figure 3C). Such overlapping pattern suggests that the two proteins may collaborate functionally in vivo. This expression data are consistent with data suggesting that simultaneous expression of zPOMT1 and zPOMT2 is required for POMT enzymatic activity. Interestingly, similar co-expression of *POMTs* was observed in various tissues and during different developmental stages of embryogenesis in mouse and *Drosophila* (Ichimiya et al. 2004; Lyalin et al. 2006; Lommel et al. 2008). These results suggest that both protein *O*-mannosylation machinery and biological importance of protein *O*-mannosylation may have been conserved during metazoan evolution, although further analyses are necessary to understand the molecular mechanisms of protein *O*-mannosylation and its evolution.

The expression levels of the two *POMTs* genes differed at various developmental stages and in specific tissues of mouse, *Drosophila* and zebrafish. For example, while mouse *POMT2* was highly expressed in testis (Willer et al. 2002), *zPOMT1* and *zPOMT2* were highly expressed in ovary and testis (Figure 3B). Since *POMT1* knockout in mice results in embryonic lethality, protein *O*-mannosylation is necessary for normal development (Willer et al. 2004). In the case of *Drosophila POMTs*, the expression level of *dPOMT1* was higher than that of *dPOMT2* from 0 to 2 h in the embryo (Ichimiya et al. 2004), whereas the expression level of *zPOMT2* was higher than that of *zPOMT1* at from 0 to 6 hpf. It was assumed that both *zPOMT1* and *zPOMT2* mRNAs at these stages were derived

from maternal expression. Furthermore, the expression level of *zPOMT1* decreased from 0 to 6 hpf, whereas *zPOMT2* expression was high from 0 to 6 hpf (Figure 3A). These results suggest that the expression of *zPOMT1* and *zPOMT2* may be regulated differently.

In humans, defects of protein *O*-mannosylation lead to WWS (Manya et al. 2003; Akasaka-Manya et al. 2004). To understand the importance of protein *O*-mannosylation in zebrafish development, we carried out the knockdown analysis of antisense MOs against *zPOMT1* and *zPOMT2*. As a result, *zPOMT1* and *zPOMT2* morphant embryos showed curved tail, and some had edematous pericardium (Figure 4B). Since both *zPOMT1* and *zPOMT2* morphants showed these phenotypic aberrations, they could not swim straight or feed at all, and they eventually died. At 96 hpf, the phenotypes of *zPOMT2* morphant embryos showed a higher incidence of more severe phenotypes than the *zPOMT1* morphant embryos did (Table I), yet immunoreactivity of IIH6 in *zPOMT1* and *zPOMT2* morphants was similar (Figure 4C). We predicted that the phenotypes of zebrafish embryos injected with MOs against *zPOMT1* and *zPOMT2* would be the same or similar because the expression patterns of the two genes were similar before 24 hpf (Figure 3). Therefore, the difference of phenotypes observed between *zPOMT1* and *zPOMT2* morphants in early development of the zebrafish might be explained by the variance of knockdown efficiency or by another function of zPOMT2 in addition to enzymatic activity. It may be consistent with severe phenotypes observed in *zPOMT2* embryos that only *zPOMT2* morphant embryos showed aberrant pigmentation in eyes. Fukutin-deficient chimeric mice revealed abnormalities in eyes, indicating that corneal opacification with vascular infiltration and eye abnormality was quite remarkable according to their aberrant pigmentation (Takeda et al. 2003). Further studies are necessary to reveal the role of *O*-mannosylglycans in the pathogenesis of eye abnormalities.

Here, we demonstrated that zebrafish POMTs possess protein *O*-mannosyltransferase activity when co-expressed in HEK293T cells. This result suggested that the protein *O*-mannosylation machinery is conserved in mammals and zebrafish. Therefore, to elucidate whether the function and mechanism of protein *O*-mannosylation related to *POMTs* are evolutionarily conserved in the vertebrates, the zebrafish should be a useful model. It was also suggested that the zebrafish may be a useful model for understanding the functions of glycans in the whole body. In the knockdown analyses of *zPOMT1* and *zPOMT2* by MOs, no glycosylated α-DG was detected in 48 hpf embryos (Figure 4C). Therefore, it appears that the enzymatic activity was completely lost. Furthermore, zebrafish α-dystroglycanopathy models may be useful to search for chemicals that treat α-dystroglycanopathies; the simple addition of candidate molecules to water could be developed as assays for theraputic effectiveness.

Materials and methods

Zebrafish and embryos

Zebrafish adults were maintained at 28°C under light condition of 14 h light period and 10 h dark period. Embryos were collected from pair-wise mating of adults and kept in filter-sterilized fresh water at 28°C.

Cloning and sequencing of the full-length cDNAs

Total RNAs were purified from 24 and 48 hpf embryos by using QIAzol (Qiagen, Hilden, Germany), and cDNA fragments were generated by RT-PCR using oligo dT primer and Superscript II reverse transcriptase (Invitrogen Corp., Carlsbad, CA). Degenerated oligonucleotide primers were designed by mRNA sequence of zebrafish POMT1 (zPOMT1) (accession no. NM_001048067.2). zPOMT2 gene (accession no. AB281276) was cloned in a zebrafish embryonic cDNA library that was synthesized with a SMART cDNA Library Construction Kit (Clontech, Mountain View, CA). Both zPOMT1 and zPOMT2 genes were amplified with the forward primers, 5′-atgcagtgtgttaaactgcccgtcagtgt-3′ and 5′-atggatgtcagaccgaaggagaatttc-3′, and the reverse primers, 5′-ttagcgtttgcgtaagagaatatcccaactctc-3′ and 5′-ctaaaactcccaggattccatccacc-3′, respectively. The amplified cDNA fragments were cloned into pT7Blue vector (Novagen, Madison, WI), and the sequences were confirmed by CEQ™ 2000 DNA Analysis System (Beckman Coulter, Inc., Fullerton, CA) with a DTCS Quick Start kit (Beckman Coulter, Inc.). The nucleotide sequence was subjected to the basic local alignment with a BLAST search provided by the National Center for Biotechnology Information. The sequences were obtained from GenBank and aligned using CLUSTAL W (Thompson et al. 1994). A phylogenetic tree was generated using the neighbor-joining method. TREEVIEW software generated visual representations of clusters (Page 1996).

Quantitative PCR analyses

Total RNA was extracted from embryos at 0, 6, 12, 18, 24, 48, 72 and 96 hpf and the tissue samples (brain, heart, liver, kidney, spleen, intestine, muscle, testis and ovary) of either male or female adult zebrafish. One microgram of total RNA was used for cDNA synthesis. First-strand cDNA was synthesized as described in the section of *cDNA cloning and sequencing of zPOMT1 and zPOMT2*. Quantitative PCR was carried out with SYBR Green Realtime PCR Master Mix (TOYOBO Co. LTD., Osaka, Japan). Two microliters of cDNA (0.1 μg/μL) was used for a template. The primers used to detect the messages of *zPOMT1* and *zPOMT2* were 5′-tgttggctgtgctgtcttacc-3′ (forward) and 5′-catggctcaaggttcgatctc-3′ (reverse), 5′-cctcatgtatgttgggatgagac-3′ (forward) and 5′-gaaccaagagcagcacagaac-3′ (reverse), respectively. The primers for *zβ-actin2* and *zCox1*—5′-agttcagccatggatgatgaaa-3′ (forward) and 5′-accatgacaccctgatgtct-3′ (reverse), 5′-ttggccacccagaagtctac-3′ (forward) and 5′-gctcgggtgtctacatccat-3′ (reverse), respectively—were used as internal controls. Annealing temperatures were 63°C for *zPOMT1* and *zPOMT2*, 52°C for *zβ-actin2* and 54°C for *zCox1*. Melting curves were calibrated by LineGene (NIPPON Genetics Co. LTD., Tokyo, Japan).

Whole-mount in situ hybridization

Antisense probe synthesis was performed using a Digoxigenin (DIG) RNA Labeling Kit (Roche Diagnostics, Basel, Switzerland). Zebrafish embryos were collected after spawning and maintained at 28°C. Embryos at 0, 6, 12, 18, 24, 48, 72 and 96 hpf were fixed with 4% paraformaldehyde (PFA)-phosphate-buffered saline (PBS), dehydrated and kept in methanol